2005-12

Performance of orthogonal frequency division multiplexing in a high noise, low signal-to-noise ratio environment with co-channel interference

Grant, Andrew G.

Monterey, California. Naval Postgraduate School

NAVAL POSTGRADUATE SCHOOL

MONTEREY, CALIFORNIA

THESIS

PERFORMANCE OF ORTHOGONAL FREQUENCY DIVISION MULTIPLEXING IN A HIGH NOISE, LOW SIGNAL-TO-NOISE RATIO ENVIRONMENT WITH CO-CHANNEL INTERFERENCE

by

Andrew G. Grant

December 2005

Thesis Advisor:	Tri Ha
Second Reader:	Herschel Loomis

Approved for public release; distribution is unlimited

THIS PAGE INTENTIONALLY LEFT BLANK

REPORT DOCUMENTATION PAGE		Form Approved OMB No. 0704-0188

1. AGENCY USE ONLY *(Leave blank)*	2. REPORT DATE December 2005	3. REPORT TYPE AND DATES COVERED Master's Thesis

4. TITLE AND SUBTITLE: Performance of Orthogonal Frequency Division Multiplexing in a High Noise, Low Signal-to-Noise Ratio Environment with Co-channel Interference	5. FUNDING NUMBERS
6. AUTHOR(S) Andrew Grant	
7. PERFORMING ORGANIZATION NAME(S) AND ADDRESS(ES) Naval Postgraduate School Monterey, CA 93943-5000	8. PERFORMING ORGANIZATION REPORT NUMBER
9. SPONSORING /MONITORING AGENCY NAME(S) AND ADDRESS(ES) N/A	10. SPONSORING/MONITORING AGENCY REPORT NUMBER

11. SUPPLEMENTARY NOTES The views expressed in this thesis are those of the author and do not reflect the official policy or position of the Department of Defense or the U.S. Government.

12a. DISTRIBUTION / AVAILABILITY STATEMENT Approved for public release; distribution is unlimited	12b. DISTRIBUTION CODE

13. ABSTRACT (maximum 200 words)

Orthogonal Frequency Division Multiplexing (OFDM) is fast becoming the signal modulation technique of choice for many commercial and military wireless applications. Its resilience to cochannel interference and bandwidth efficiency make it ideal for many different applications. With its increasing popularity among disparate facets of society, it becomes likelier that enemy militaries and/or nonmilitary combatants will utilize the technique or a system that uses the technique. In light of this development, the need to develop techniques and algorithms to enable detection becomes apparent. This thesis will attempt to develop a model for OFDM and measure its performance in a multipath, outdoor environment with low signal-to-noise ratio, high noise and cochannel interference. Because of the unpredictability of the outdoor environment and the proliferation of various OFDM standards, the simulation will utilize only one algorithm for modeling outdoor environments and the IEEE 802.11a standard.

14. SUBJECT TERMS Orthogonal Frequency Division Multiplexing. OFDM, Cochannel interference, Multipath fading, IEEE 802.11a, Rayleigh fading, Rician fading, exponential channel model	15. NUMBER OF PAGES 69
	16. PRICE CODE

17. SECURITY CLASSIFICATION OF REPORT	18. SECURITY CLASSIFICATION OF THIS PAGE	19. SECURITY CLASSIFICATION OF ABSTRACT	20. LIMITATION OF ABSTRACT
Unclassified	Unclassified	Unclassified	UL

NSN 7540-01-280-5500 Standard Form 298 (Rev. 2-89)

THIS PAGE INTENTIONALLY LEFT BLANK

Approved for public release; distribution is unlimited

PERFORMANCE OF ORTHOGONAL FREQUENCY DIVISION MULTIPLEXING IN A HIGH NOISE, LOW SIGNAL-TO-NOISE RATIO ENVIRONMENT WITH CO-CHANNEL INTERFERENCE

Andrew G. Grant
Lieutenant Commander, United States Navy
B.S., University of South Carolina, 1992

Submitted in partial fulfillment of the
requirements for the degree of

MASTER OF SCIENCE IN ELECTRICAL ENGINEERING

from the

NAVAL POSTGRADUATE SCHOOL
December 2005

Author: Andrew G. Grant

Approved by: Tri Ha
Thesis Advisor

Herschel Loomis
Second Reader

Jeffrey Knorr
Chairman, Department of Electrical Engineering

THIS PAGE INTENTIONALLY LEFT BLANK

ABSTRACT

Orthogonal Frequency Division Multiplexing (OFDM) is fast becoming the signal modulation technique of choice for many commercial and military wireless applications. Its resilience to cochannel interference and bandwidth efficiency make it ideal for many different applications. With its increasing popularity among disparate facets of society, it becomes likelier that enemy militaries and/or nonmilitary combatants will utilize the technique or a system that uses the technique. In light of this development, the need to develop techniques and algorithms to enable detection becomes apparent. This thesis will attempt to develop a model for OFDM in a multipath, outdoor environment with low signal-to-noise ratio, high noise and cochannel interference. Because of the unpredictability of the outdoor environment and the proliferation of various OFDM standards, the simulation will utilize only one algorithm for modeling outdoor environments and the IEEE 802.11a standard.

THIS PAGE INTENTIONALLY LEFT BLANK

TABLE OF CONTENTS

THIS PAGE INTENTIONALLY LEFT BLANK

LIST OF FIGURES

LIST OF TABLES

THIS PAGE INTENTIONALLY LEFT BLANK

ACKNOWLEDGMENTS

First and foremost I would like to thank my Lord and Savior Jesus Christ, without whom I would not have completed this season of my career. Secondly, I would like to thank my wife and children who encouraged me at every obstacle and celebrated with me at every victory.

I also would like to thank my thesis advisor, Dr. Tri Ha, whose patience and quiet confidence helped to keep me on the straight path. Lastly, I would like to thank Nathan Beltz who provided guidance and a plethora of invaluable advice.

THIS PAGE INTENTIONALLY LEFT BLANK

EXECUTIVE SUMMARY

Orthogonal Frequency Division Multiplexing (OFDM) describes a type of multicarrier modulation (MCM) technique formally introduced by R. W. Chang in 1966 [1], but whose antecedents can be found in the military application of the Kineplex Multicarrier High Frequency (HF) Modem in 1957. The difference between simple MCM and OFDM resides primarily in the latter's requirement for the frequencies to be orthogonal, i.e. noninterfering. In 1971 Weinstein and Ebert proposed using the Fast Fourier Transform (FFT) to eliminate the need for a bank of local oscillators and a guard interval to prevent intersymbol interference (ISI). However, it was not until the 1990s when Very Large Scale Integration (VLSI) circuit technology advanced enough to make large scale FFTs possible and, hence, large data rates feasible for OFDM. Currently OFDM is being considered for the Joint Tactical Radio System (JTRS) and is the standard for the Asymmetrical Digital Subscriber Line (ADSL), Digital Audio Broadcasting (DAB) - the first OFDM based standard, Digital Video Broadcasting (DVB), in local area networks (LAN) and others.

Qualitatively, OFDM takes an information bit, maps it to a symbol, which describes it in terms of its in-phase and quadrature components. This is then translated to the time domain through the use of an inverse FFT (IFFT), converted to an analog signal, and transmitted by quadrature modulation. The subcarriers of OFDM are orthogonal; therefore, the subcarriers do not interfere with each other. The receiver performs substantially the same operation in reverse.

The ubiquitous nature of OFDM makes it necessary to determine its performance in many different environments. This thesis sought to determine that performance in an indoor or outdoor environment. The thesis also took into account different types of multipath fading. Both Rayleigh and Rician fading were modeled. The presence of cochannel interference is a very real possibility since IEEE 802.11a operates in an unregulated bandwidth. The channel model used in the thesis also allows cochannel interference to be included in performance analysis, and this was also considered. Finally

the thesis considers the effect of varying root mean square delay spreads. Time dispersion can vary across a wide range depending upon the operating environment. The inclusion of various interferers in the performance analysis showed significant degradation in performance.

I. INTRODUCTION

Orthogonal Frequency Division Multiplexing (OFDM) describes a type of multicarrier modulation (MCM) technique formally introduced by R. W. Chang in 1966 [1], but whose antecedents can be found in the military application of the Kineplex Multicarrier High Frequency (HF) Modem in 1957. The difference between simple MCM and OFDM resides primarily in the latter's requirement for the frequencies to be orthogonal, i.e. noninterfering. In 1971 Weinstein and Ebert proposed using the Fast Fourier Transform (FFT) to eliminate the need for a bank of local oscillators and a guard interval to prevent intersymbol interference (ISI). However, it was not until the 1990's when Very Large Scale Integration (VLSI) circuit technology advanced enough to make large scale FFTs possible and, hence, large data rates feasible for OFDM. Currently OFDM is being considered for the Joint Tactical Radio System (JTRS) and is the standard for the Asymmetrical Digital Subscriber Line (ADSL), Digital Audio Broadcasting (DAB) - the first OFDM based standard, Digital Video Broadcasting (DVB), local area networks (LAN) and others.

Because of its increasing popularity, particularly in the realm of LANs, two standards have emerged for its implementation: High Performance Radio LAN (HiperLAN)/2 and Institute of Electrical and Electronic Engineers (IEEE) 802.11a. HiperLAN/2 is a standard developed by the European Telecommunications Standards Institute. IEEE 802.11a is the predominant wireless LAN standard, although it does share some similarities with HiperLAN/2 up to the medium access control layer (MAC).

Qualitatively, OFDM takes an information bit, maps it to a symbol, which describes it in terms of its in-phase and quadrature components. This is then translated to the time domain through the use of an inverse FFT (IFFT), converted to an analog signal, mixed, and transmitted. The receiver performs substantially the same operation in reverse.

This technique has several advantages. Unlike, frequency division multiplexing, the multiple carriers can be squeezed together due to their orthogonality, thereby increasing the bandwidth efficiency.

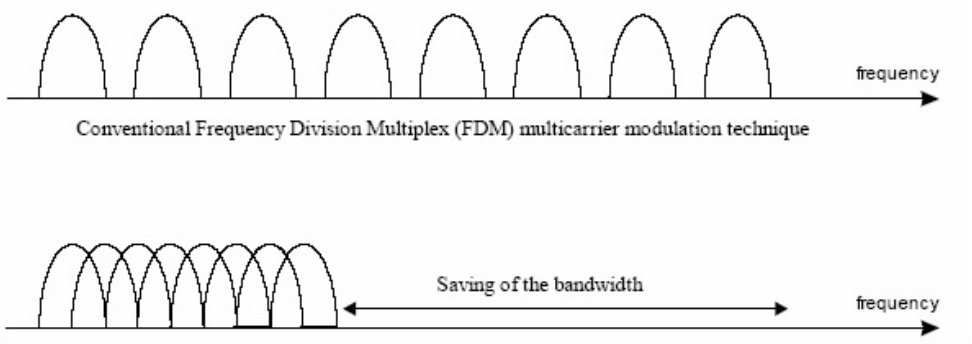

Figure 1. Bandwidth use comparison in FDM and OFDM (From Ref.[2])

Another advantage of OFDM is its resistance to multipath delay spreading or fading, hence, its great use in LANs. Multipath fading presents a great problem in urban canyons and in non line of sight (LOS) environments. The fading comes from the radio signal taking an indirect path to the receiver, e.g. reflecting off buildings, vehicles, foliage, and people. These signals may eventually reach their intended destination, but late and/or distorted. Signals that arrive late may even add destructively or constructively. This variation in signal amplitude is fading. The amount of fading depends upon the environment. OFDM distributes bits across multiple tones and sends a smaller amount of information at any particular frequency. This produces a flat channel frequency response.

A. OBJECTIVE

The objective of this thesis is to discuss and simulate an OFDM signal's performance in a high noise, low signal power and cochannel interference and to determine the probability of accurate retrieval of the signal. The model takes into account some of the major causes of OFDM degradation, e.g. multipath fading, phase noise, and frequency offset.

B. THESIS OUTLINE

This thesis provides an overview of OFDM basics, in general, and the IEEE 802.11a standard, in particular, followed by a quick survey of multipath fading in an outdoor environment. The reader is then shown the channel modeling and actual realization.

This thesis is organized as follows:

Chapter II discusses OFDM basics and the IEEE 802.11a physical layer. It also covers the problems of multipath fading and cochannel interference.

Chapter III takes an in-depth look at the channel model utilized for conducting the simulations.

Chapter IV emphasizes the algorithms and Matlab coding techniques utilized for the simulations. Several operational modes of IEEE 802.11a are evaluated with different operating modes and under different channel environments.

Chapter V summarizes the research and provides consideration for future research.

THIS PAGE INTENTIONALLY LEFT BLANK

II. BACKGROUND

As noted above, the concept of OFDM finds its genesis in the mulitcarrier modulation techniques postulated by R. W. Chang in 1966, but only in the last decade has it become technologically feasible to make use of this technique. OFDM's advantages over single-carrier modulation techniques include more efficient bandwidth utilization and higher data rates.

This chapter will discuss OFDM and the IEEE 802.11a standard. It will also discuss some of the performance impairments unique to the wireless environment, e.g. multipath fading. The chapter includes a discussion of the outdoor wireless environment.

A. OFDM OVERVIEW

Two signals are orthogonal over a period *T* when the integral of their product over *T* is zero as described by

$$\int_0^T x(t)y(t)dt = 0. \tag{0.1}$$

The carriers of an OFDM signal are mutually orthogonal because each sinusoid is a multiple of a fundamental frequency. This orthogonality allows multiple signals to be placed closely together within the assigned bandwidth. For example, the required null-to-null bandwidth for a binary phase-shift keying (BPSK) signal using a data rate of 6 Mbps and a rate-1/2 encoding scheme requiring a total coded data rate of 12 Mbps uses a 24 MHz bandwidth. However, this same signal transmitted using the IEEE 802.11a OFDM modulation uses only 16.6 MHz of bandwidth. Figure 2 shows the spectrum of five OFDM subchannels.

Notice also in Figure 2 that the spectral peak of each subchannel coincides with a null of the other carriers. Therefore, the difference between the center lobe and the first zero crossing represents the minimum required spacing and is equal to 1/T [3]. This method avoids intercarrier interference.

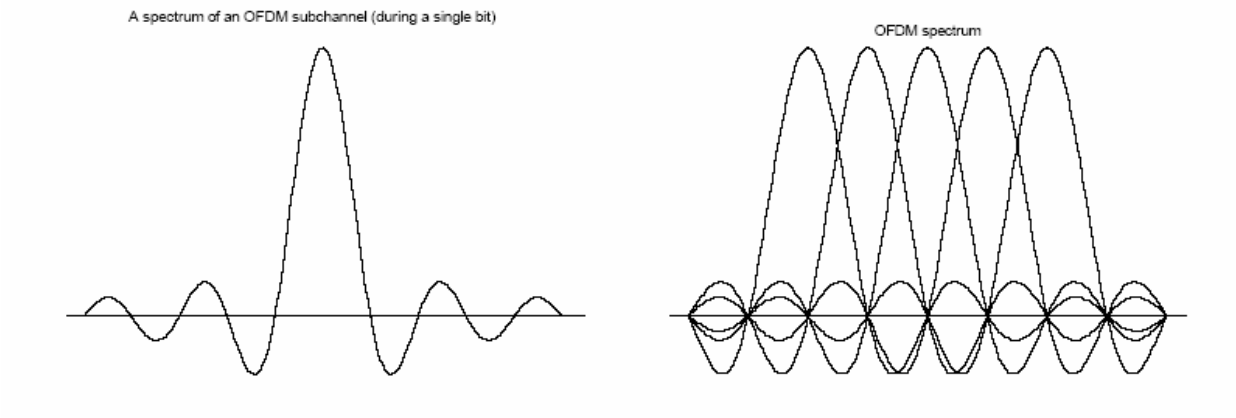

Figure 2. OFDM Spectrum-Single bit and five bits (From Ref. [1])

To reduce the effects of intersymbol interference (ISI), all the orthogonal subcarriers are transmitted simultaneously. The narrow orthogonal subcarriers occupy the entire allocated bandwidth. The transmission of several symbols in parallel lengthens the symbol duration, which reduces the ISI effects caused by the dispersive multipath fading environment [4].

The basic OFDM transmitter is straightforward. Figure 3 below provides an overview of an OFDM transmitter. Data, as represented in binary, is demultiplexed by a

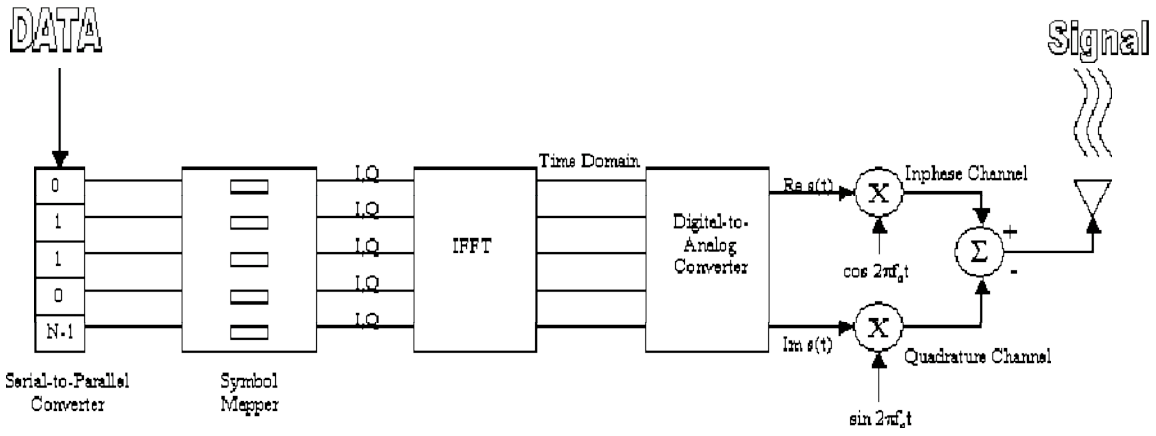

Figure 3. Basic OFDM Transmitter

serial-to-parallel converter and mapped to a symbol. The symbol mapper represents the data by its inphase and quadrature (IQ) components. At this point the signal is said to be in the frequency domain from the point of FFT/IFFT jargons. An inverse discrete Fourier

transform (IDFT) takes the frequency domain IQ components and converts them to time domain samples. The discrete Fourier transform (DFT) and the IDFT are defined, respectively, as

$$X(k) = \sum_{n=0}^{N-1} x(n) \bullet e^{-j2\pi kn/N} \tag{0.2}$$

$$x(n) = \frac{1}{N} \sum_{k=0}^{N-1} X(k) \bullet e^{j2\pi kn/N} \tag{0.3}$$

In practice, the Fast Fourier Transform (FFT) and the Inverse Fast Fourier Transform (IFFT) are utilized.

A digital-to-analog (D/A) converter allows the digital representation to be modulated onto a carrier for transmission. The symbol rate for each carrier is 1/NT (symbols/sec), where N is the number of IFFT bins and T is the time sampling period. Each subcarrier frequency is separated by an integer multiple of 1/NT (Hz). Any modulation technique, for example, binary phase shift keying (BPSK), Quadrature Amplitude Modulation (QAM), can be used with each symbol sent in OFDM, although, practically, only one is used.

The OFDM receiver performs, essentially, the opposite functions. The signal is demodulated and separated into its real and imaginary components through an inphase-quadrature demodulator. Those components are then converted into their digital representation. Next it is sent through an FFT, which converts the signal into the frequency domain. Each part of the signal, i.e. each symbol, is now defined by its inphase and quadrature coordinate. The symbol demapper then produces an output corresponding to a particular symbol that then goes through a parallel-to-serial converter whose output is the original data.

Transmission channel distortion prevents the consistent maintenance of orthogonality. The distortion due to multipath fading causes each subcarrier to spread the power into the adjacent subcarriers. Both intersymbol interference (ISI) and intercarrier

interference (ICI) are likely to occur. To reduce the distortion it is necessary to increase the symbol duration or the number of carriers.

A cyclically extended guard interval (GI) illustrates one way to eliminate ISI. Figure 4 shows cyclic prefix method. Each OFDM symbol is preceded by a periodic extension of the signal itself [3].

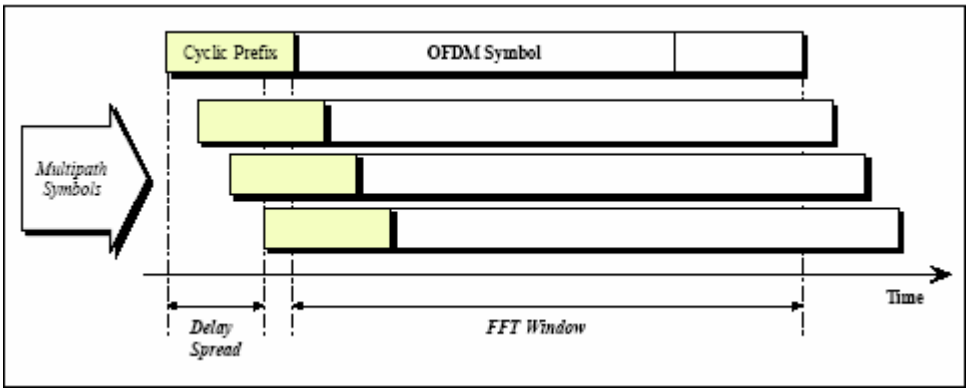

Figure 4. Cyclic Prefix (CP)in OFDM Symbol (From Ref.[5])

The total symbol duration is

$$T_{total} = T_{gi} + T_s, \tag{0.4}$$

where T_{gi} is the guard interval.

Each symbol's duration is made of two parts. The whole signal is also repeated at the start of the symbol and is called the guard interval or cyclic prefix. When the CP is longer than the channel impulse response (CIR), or the multipath delay spread, the effect of ISI can be eliminated; however, ICI still exists.

The GI length depends upon the application. When designing a system, the designer must consider the loss of bandwidth that accompanies GI usage. Tgi is usually selected to be one-fourth of the OFDM symbol period [6].

B. IEEE 802.11A STANDARD

The goal of the IEEE 802.11 standard promulgated in 1997 describes a wireless local area network (WLAN) that delivers services previously found only in wired

networks, e.g., high throughput, highly reliable data delivery, and continuous network connections [7]. The 802.11a physical layer (PHY) utilizes a wireless transmission medium and operates in the 5 GHz frequency range [8].

1. PHY Specifications

The IEEE 802.11a standard differs from the 802.11 standard in that it utilizes OFDM as the means of modulation. Figure 5 provides an overview of the OFDM PHY architecture.

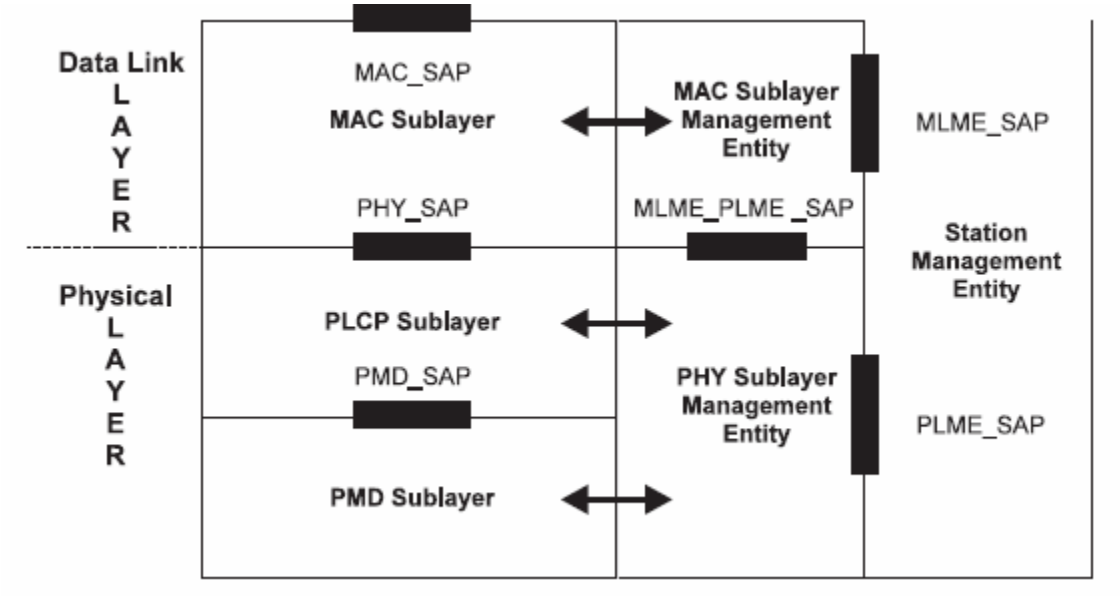

Figure 5. IEEE 802.11 Basic Reference Model (From Ref. [8])

It contains three functional entities: the physical medium dependent (PMD) system, the PHY convergence function, and the layer management function. The PMD sublayer provides a means to send and receive data between two or more stations. The PHY convergence function adapts the capabilities of the PMD. The layer management function manages the local PHY functions. Other elements of the Figure 5 will be discussed in Section 2.

Data rate (Mbits/s)	Modulation	Coding rate (R)	Coded bits per subcarrier (N_{BPSC})	Coded bits per OFDM symbol (N_{CBPS})	Data bits per OFDM symbol (N_{DBPS})
6	BPSK	1/2	1	48	24
9	BPSK	3/4	1	48	36
12	QPSK	1/2	2	96	48
18	QPSK	3/4	2	96	72
24	16-QAM	1/2	4	192	96
36	16-QAM	3/4	4	192	144
48	64-QAM	2/3	6	288	192
54	64-QAM	3/4	6	288	216

Table 1. Rate-dependent Parameters of IEEE 802.11a (From Ref. [8])

The allowed data rates are 6, 9, 12, 18, 24, 36, 48, and 54 Mbps. Table 1 and Table 2 contain the key parameters.

Parameter	Value
N_{SD}: Number of data subcarriers	48
N_{SP}: Number of pilot subcarriers	4
N_{ST}: Number of subcarriers, total	52 ($N_{SD} + N_{SP}$)
Δ_F: Subcarrier frequency spacing	0.3125 MHz (=20 MHz/64)
T_{FFT}: IFFT/FFT period	3.2 μs ($1/\Delta_F$)
$T_{PREAMBLE}$: PLCP preamble duration	16 μs ($T_{SHORT} + T_{LONG}$)
T_{SIGNAL}: Duration of the SIGNAL BPSK-OFDM symbol	4.0 μs ($T_{GI} + T_{FFT}$)
T_{GI}: GI duration	0.8 μs ($T_{FFT}/4$)
T_{GI2}: Training symbol GI duration	1.6 μs ($T_{FFT}/2$)
T_{SYM}: Symbol interval	4 μs ($T_{GI} + T_{FFT}$)
T_{SHORT}: Short training sequence duration	8 μs ($10 \times T_{FFT}/4$)
T_{LONG}: Long training sequence duration	8 μs ($T_{GI2} + 2 \times T_{FFT}$)

Table 2. Timing-related Parameters IEEE 802.11a (From Ref. [8])

The 802.11a standard allows binary or quadrature phase-shift keying (BPSK/QPSK), 16 or 64 Quadrature Amplitude Modulation (QAM) of 52 subcarriers. The error correcting code is 64-state convolutional code with coding rates of 1/2, 2/3, or 3/4. It occupies 16.6 MHz bandwidth with an OFDM symbol duration of 4.0μs and T_{gi}=0.8μs.

2. OFDM PHY Architecture

The OFDM PHY is comprised of two elements: the Physical Layer Convergence Protocol (PLCP) and the Physical Medium Dependent (PMD) sublayers. The PHY transmits Medium Access Control (MAC) Protocol Data Units (MPDUs) as the MAC layer directs.

The PLCP transmit procedure is illustrated in Figure 6. The MAC layer communicates with the PLCP through a PHY service access point. Once the MAC makes the request, the PLCP prepares the MPDU for transmission by adding a header and tail bits. The MPDU becomes a PHY Service Data Unit (PSDU). The PSDU and tail bits are scrambled and encoded by a convolutional encoder.

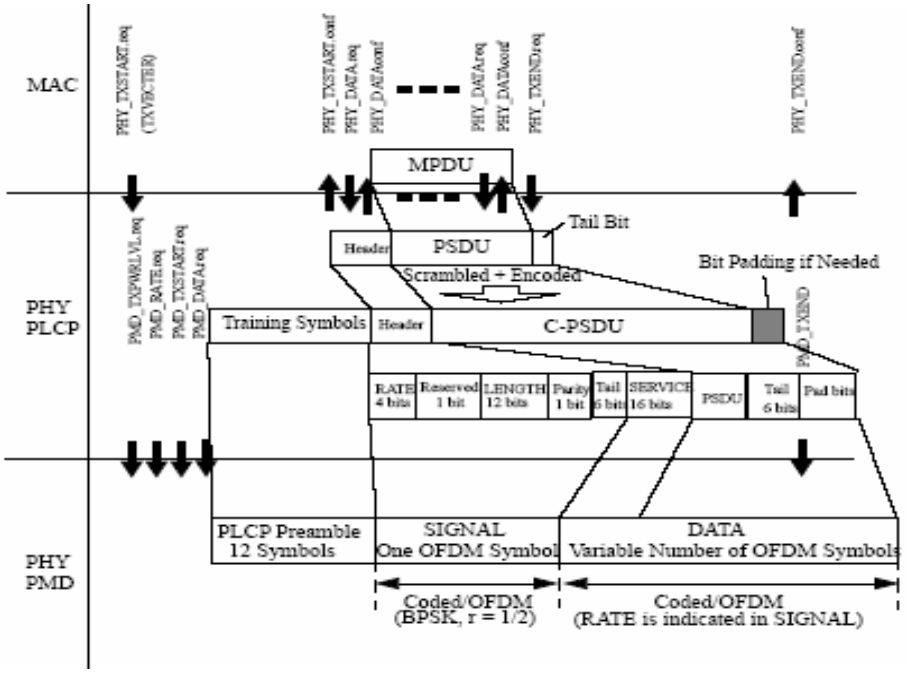

Figure 6. PLCP Transmit Procedure in IEEE 802.11a (From Ref. [8])

The PLCP transmission begins with the coded PSDU (CPSDU). The PHY PLCP adds bits to the CPSDU if it is not multiples of the OFDM symbol. Finally, in the PMD, the PLCP Protocol Data Unit (PPDU) is formed. It consists of the PLCP Preamble, the SIGNAL, and the DATA. Figure 7 illustrates the entire 802.11a OFDM training structure.

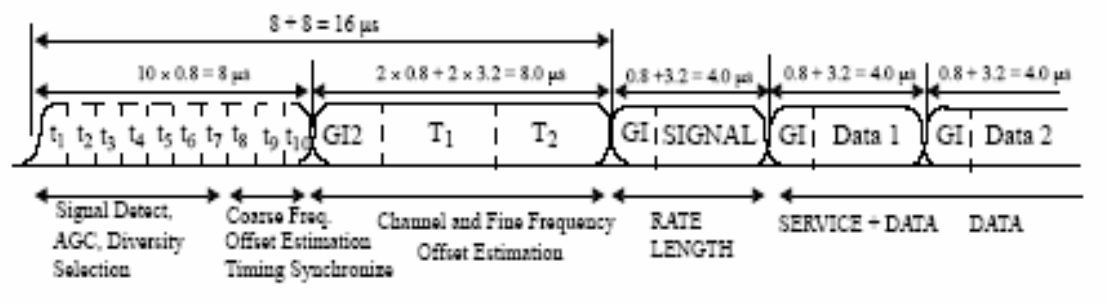

Figure 7. Training structure (From Ref. [8])

The PLCP preamble field consists of 10 short symbols (12 subcarriers) and two long symbols (53 subcarriers) used for synchronization. The first seven short training symbols are for signal detection, automatic gain control (AGC), and diversity selection. The final three short symbols are for coarse frequency estimation and timing synchronization. The long symbols are for channel and fine frequency offset estimation.

The composition of the SIGNAL field consists of 24 bits. The first four bits encode the rate as enumerated above in Table 1. The fifth bit is reserved. Bits five through 16 encode the number of bytes in the PSDU. Bit 17 is a parity bit. Bits 18 through 23 constitute the SIGNAL tail and are set to zero.

The DATA field contains 22 or more bits made of the service field, the PSDU, the tail bits, and the pad bits if necessary.

The PLCP specifies how the PMD entity will impose the signals onto the medium. In other words, the PMD entity actually interfaces with the medium and receives/transmits transmissions between stations.

3. The MAC Layer

The MAC layer provides three functions in the IEEE 802.11a standard [7]:

- Provide a reliable data delivery service. The IEEE 802.11 MAC improves on the reliability of data delivery over wireless media through a frame exchange protocol.
- Fairly control access to the shared wireless medium. It performs this through the basic access mechanism, called the distributed coordination function, and a centrally controlled access mechanism, called the point coordination function.
- Protect the data it delivers. The MAC encrypts the data through its Wired Equivalent Privacy (WEP).

The basic access mechanism is carrier sense multiple access with collision avoidance (CSMA/CA). The station listens to the medium before transmitting to determine whether or not it is already in use. If it is not in use, the station will broadcast. This avoids collisions in the medium.

C. SIGNAL PROPAGATION

Wireless communications bring a host of advantages, including mobility, less clutter, convenience. It also makes communications more complex. Unlike wired communications where the communication path is controlled, in part, by the medium, wireless media allow the signal to go everywhere, taking multiple paths to the intended receiver. These multiple paths distort the signal due to reflection, diffraction and scattering.

The multipath propagation causes the received signal to consist of an infinite sum of attenuated, delayed, and phase-shifted replicas of the transmitted signal [9]. The multipath components arrive at the receiver with varying amplitudes and a random phase relationship that continuously changes due to movement of the receiver, the transmitter and objects in the environment. This causes rapid fluctuations in signal strength that are superimposed on the large scale path loss associated with distance between the

transmitter and receiver. As illustrated in Figure 8, these different paths, including a line of sight path, may be modeled with a single-channel model, where the multiple paths have different delays and attenuations.

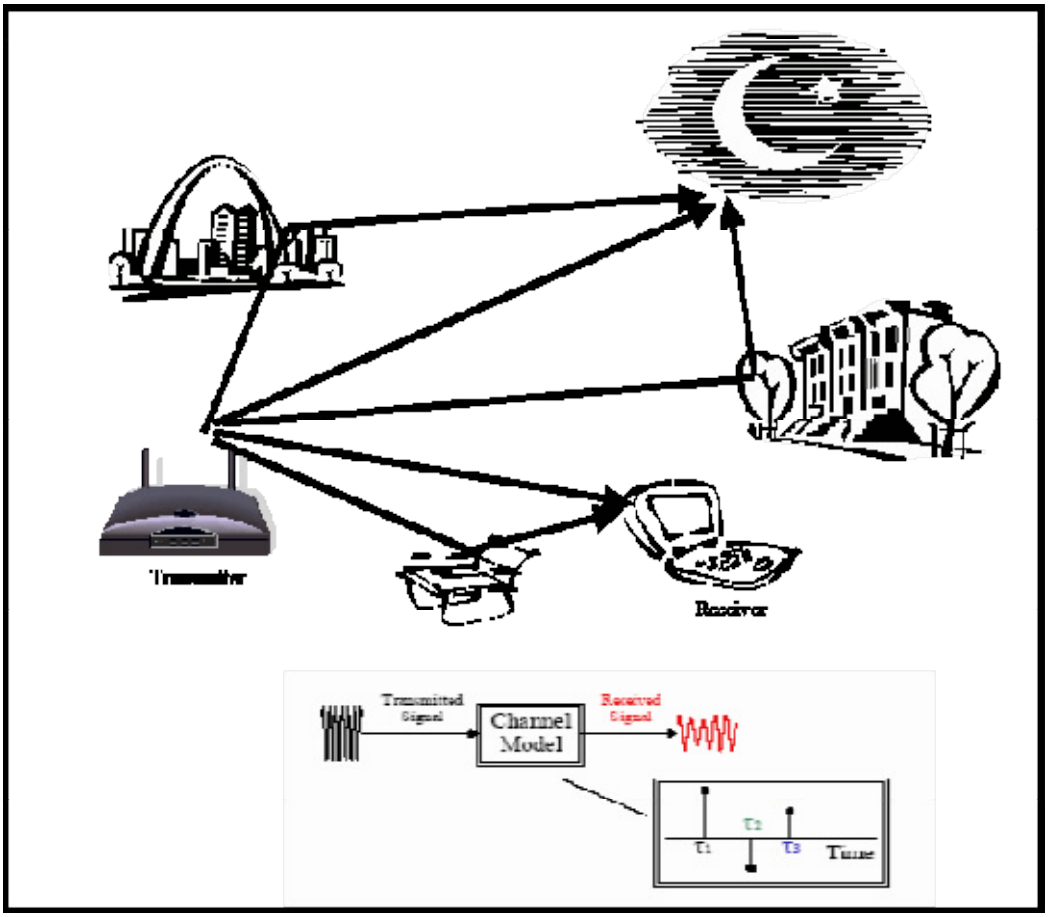

Figure 8. Multipath Propagation (After Ref. [5])

The delay and attenuation of the signal usually corresponds to the length of the path traveled, but other factors such as partial absorption by the reflector can further attenuate the signal. When the replicated signals arrive concurrently, but out of phase, they may add destructively. If this destructive combining occurs, the signal experiences fading.

The near impossibility of predicting the small scale variations in signal strength requires modeling based upon stochastic processes. In environments where the LOS

component is blocked the Rayleigh process provides a suitable model. When a LOS component is present, the Rician process provides a more suitable model [3].

1. Large Scale Path Loss

Two types of fading effects attenuate a transmitted signal: large scale fading and small scale fading. Large scale fading is the effect of simple path loss. The signal is attenuated by a factor of $\overline{L_p}(\mathrm{d})$ [10]. $\overline{L_p}(\mathrm{d})$ indicates the mean path loss and is proportional to an nth-power of d relative to a reference distance, d_o, corresponding to a point in the far field of the antenna and is describe by

$$\overline{L_p}(d) \propto \left(\frac{d}{d_o} \right)^n .$$

The path loss exponent, n, depends on the environment, frequency, and antenna heights.

Figure 9 shows the path loss values measured for different distances. Curves are superimposed for a log-distance model with n=1 through n=5, with the average path loss corresponding to n=2.7 and the standard deviation σ=11.8 dB. If the data is assumed to be Gaussian distributed, then greater than 90 percent of measured path loss values fall within $\pm 2\sigma$ ($\pm$ 23.6 dB) of the average path loss.

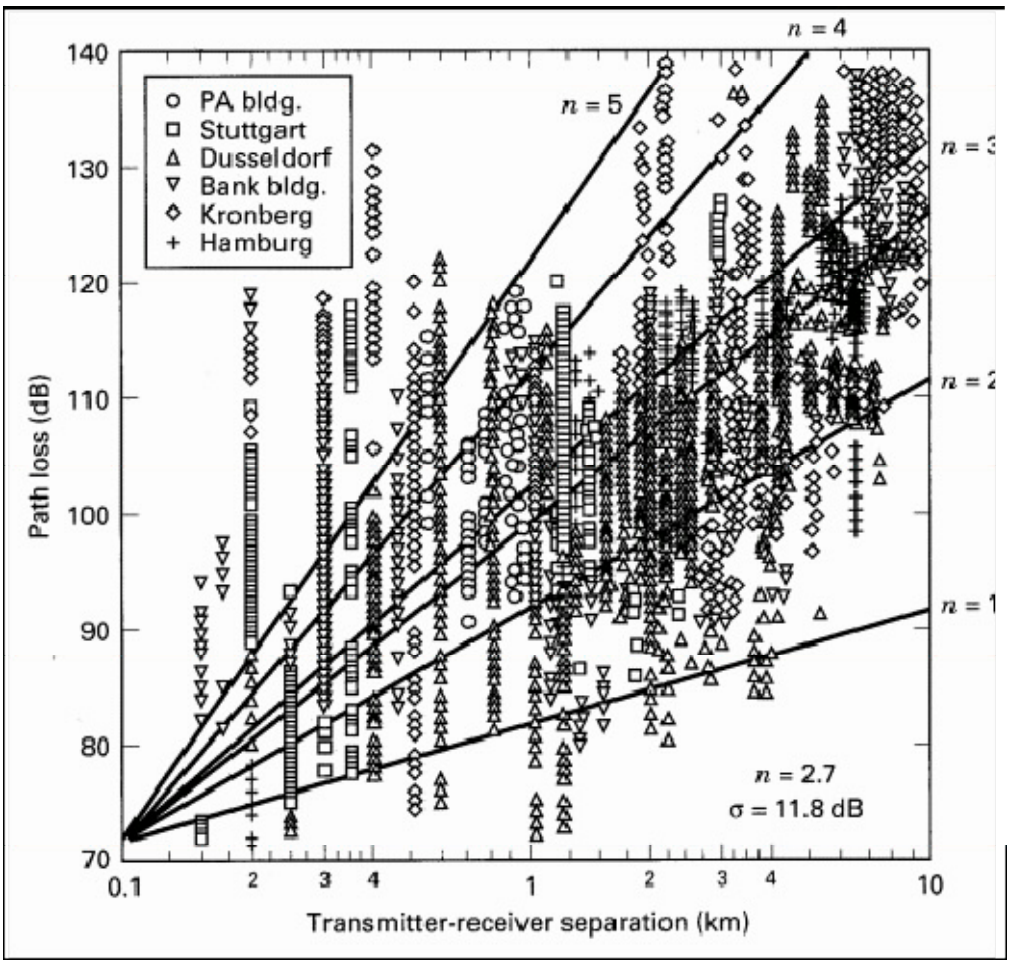

Figure 9. Path Loss vs. Distance (From Ref. [10])

2. Small Scale Fading and Multipath

Since both the delay and attenuation of a transmitted signal vary, random processes must be employed to model them. A random process can be described by its autocorrelation function in the time and frequency domains [12]

$$R_{hh}(\tau_1,\tau_2;t_1,t_2)=\frac{1}{2}E\left\{h^*(\tau_1;t_1)h(\tau_2;t_2)\right\}, \tag{0.5}$$

$$R_{HH}(f_1,f_2;t_1,t_2)=\frac{1}{2}E\left\{H(f_1;t_1)H^*(f_2;t_2)\right\} \tag{0.6}$$

where $h(\tau;t)$ is the channel's time varying impulse resonse, and $H(f;t)$ is the Fourier transform of $h(\tau;t)$ with respect to time difference of arrival τ.

It can be shown that an adequate model for the fading in the channel is the wide sense stationary uncorrelated scattering (WSSUS) [13]. Bello showed that the mobile channel was invariant under a translation in time; therefore, the autocorrelation functions depended only upon the difference in time (wide sense stationary). He also showed that for most channels the contributions of scattering from elements having different time delays is uncorrelated [13]. The description of the channel by the autocorrelation function, R_{hh}, becomes [12]:

$$R_{hh}(\tau_1, \tau_2; \Delta t) = \delta(\tau_1 - t_2) P_h(\tau_1; \Delta t). \tag{0.7}$$

The Fourier transform relation between $R_{hh}(\tau_1,\tau_2;\Delta t)$ and $P_h(\tau_1;\Delta t)$ is

$$P_h(\tau; \Delta t) = \int_{-\infty}^{\infty} R_{HH}(\Delta f; \Delta t) e^{j2\pi\tau(\Delta f)} d(\Delta f), \tag{0.8}$$

which describes the inverse Fourier transform of $R_{HH}(\Delta f; \Delta t)$ with respect to Δf. $P_h(\tau; \Delta t)$ is the power spectral density of the signal.

The multipath intensity profile describes how the average received power varies with time. Figure 10 shows a multipath intensity profile (MIP) done in Aarhus and

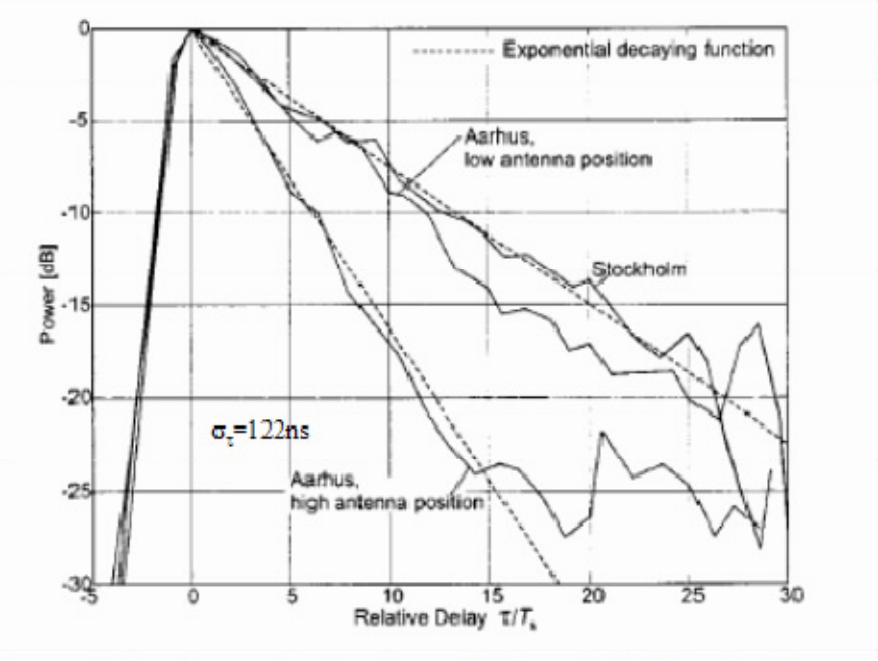

Figure 10. Multipath Intensity Profile (From Ref. [14])

Stockholm, Sweden. The root mean square (RMS) delay spread is 122 ns. Over this period the MIP is non-zero.

The RMS delay spread denotes the spreading of the narrow pulse measured in terms of the standard deviation and is more widely used than the mean excess delay ($\bar{\tau}$). The mean excess delay is the first moment of the power delay profile and is defined as [15]:

$$\bar{\tau} = \frac{\sum_{\kappa} P(\tau_k)\tau_k}{\sum_{\kappa} P(\tau_k)}. \tag{0.9}$$

The RMS delay spread is the square root of the second central moment of the power delay profile and is defined as:

$$\sigma_\tau = \sqrt{\frac{\sum_{\kappa} P(\tau_k)(\tau_k - \bar{\tau})^2}{\sum_{\kappa} P(\tau_k)}}. \tag{0.10}$$

Both delays are measured relative to the first arriving signal.

Small scale fading is the effect of small changes in the relative positions of the transmitter and receiver. These effects manifest in the time spreading of the signal and time variance of the channel. Figure 11 provides a qualitative view of the small scale fading phenomena. It shows a power delay profile for an outdoor channel.

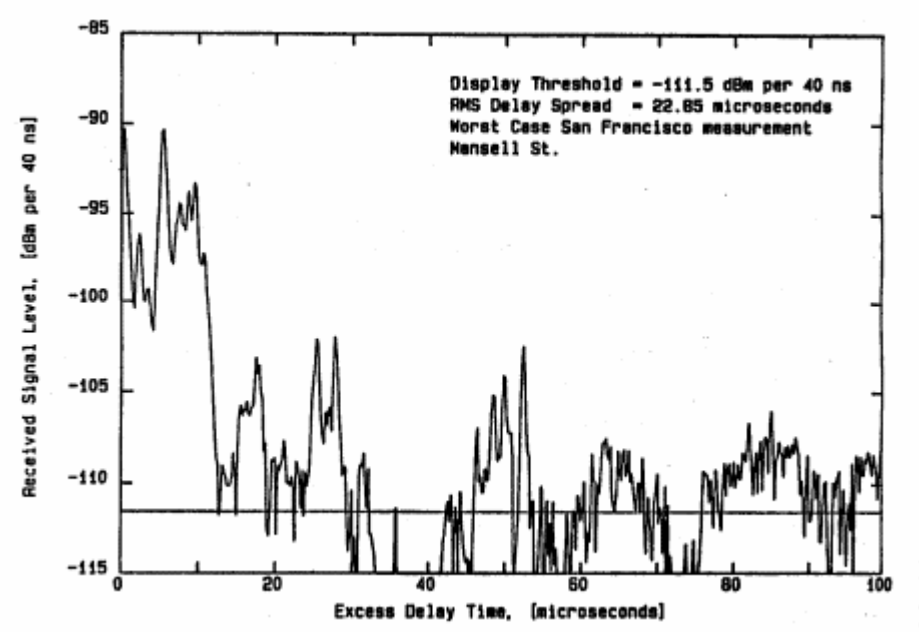

Figure 11. Reflected signal effect on desired signal (From Ref. [11])

Notice how the received signal power varies with time measured in microseconds.

Two different types of degradation occur in a fading channel as it concerns the relationship between the RMS delay spread, σ_τ, and symbol time, T_s: frequency-selective fading and frequency nonselective or flat fading [10]. Frequency-selective fading occurs when $\sigma_\tau >> T_s$ and produces intersymbol interference (ISI) [11]. In other words the symbol's components extend beyond the symbol's time duration. Flat fading occurs when $\sigma_\tau << T_s$ [11]. No ISI occurs, but phase differences can cause a reduction in SNR.

D. INDOOR VS. OUTDOOR WIRELESS ENVIRONMENT

The outdoor wireless environment differs from the indoor wireless environment in terms of modeling complexity. The indoor environment is characterized by a finite number of objects that cause multipath propagation, which can lead to degradations in the signal through attenuation and delay. The outdoor model must take into account many objects capable of the scattering, reflecting, absorbing, or shadowing the desired signal depending on the environment, e.g. rural, suburban, or urban. Also, there is a greater chance of cochannel interference (CCI). This is of great concern in mobile telephony as users move from cell to cell and greater numbers of users utilize the same frequency

spectrum. This is also a problem in the WLAN domain due to the proliferation of home LANs operating in the same unlicensed frequency range.

E. SUMMARY

This chapter discussed the basics of orthogonal frequency division multiplexing. Its advantages lie primarily in the orthogonality of the frequencies for the subcarriers. This allows the subcarriers to be overlapped within the allowable bandwidth, thereby increasing spectral efficiency.

The IEEE 802.11a standard was described. The PHY was discussed in detail. The guard interval (GI) helps mitigate ISI and maintain synchronization.

The chapter also addressed multipath fading. The signal spreading and attenuation result directly from multipath fading. The two types, frequency-selective fading and flat fading can and do occur in the same channel. Finally, a brief discussion of the outdoor wireless environment was provided.

As described in this chapter, a stochastic process can model the fading and interference. The next chapter will discuss the channel model chosen.

III. CHANNEL MODEL

Stochastic processes provide the means to realistically model wireless communication channels due to the their time varying nature. This chapter will discuss the exponential model channel approved by the IEEE Task Group b. An overview of the modifications made to that model for use in this research is discussed. Finally, the effect of cochannel interference (CCI) and its implementation are discussed.

A. EXPONENTIAL CHANNEL MODEL

The multiple propagation paths seen in wireless communications, especially those in the outdoor environment, could continue ad infinitum; however, the longer a signal takes to arrive at the receiver, the more attenuated it is. A very good technique for modeling this channel is the exponential model.

1. IEEE 802.11 Task Group B

Despite the many models available and recommended for wireless channel modeling, the IEEE Task Group b chose the exponential model because it is easy to generate and is a reasonably accurate depiction of the real world [15]. The necessity of constructing a multipath model that will allow accurate performance assessments of different waveforms for wireless LANs led to the proposal in [16].

The model is fairly straightforward. The taps are independent complex-valued zero-mean Gaussian random variables with variances (power) that decay exponentially. Although there are potentially an infinite number of taps in the exponential model, the magnitude of the taps decays rapidly. The rapid decay allows truncation of the taps, which in turn supports representation of the channel as a finite impulse response (FIR) model. The channel impulse response is [16]

$$h_k = N(0,\frac{1}{2}\sigma_k^2) + j \cdot N(0,\frac{1}{2}\sigma_k^2) \text{ for } k=0,1,\ldots,k_{max} \tag{0.11}$$

where

$$k_{\max} = \lceil 10 \cdot \tau_{rms} / f_s \rceil$$

$$\beta \triangleq e^{-f_s/\tau_{rms}}$$

$$\sigma_k^2 = \sigma_o^2 \beta^k \tag{0.12}$$

$$\sigma_o^2 = \frac{1-\beta}{1-\beta^{k_{\max}+1}}.$$

The parameter k_{max} determines the tap truncation point and it depends upon the primary parameters in the model are the RMS delay spread, τ_{RMS}, and the sampling period, f_s, (the spacing between taps). It can be shown that the last tap is [15]

$$e^{-k_{\max} f_s/\tau_{rms}} = e^{-10} \simeq 4.5\times10^{-5}, \tag{0.13}$$

which is a fairly small number. The small value of the last tap coupled with the fact that the exponential channel is decaying monotonically, leads to the conclusion that the truncation does not significantly alter the model. Figure 12 illustrates the difference

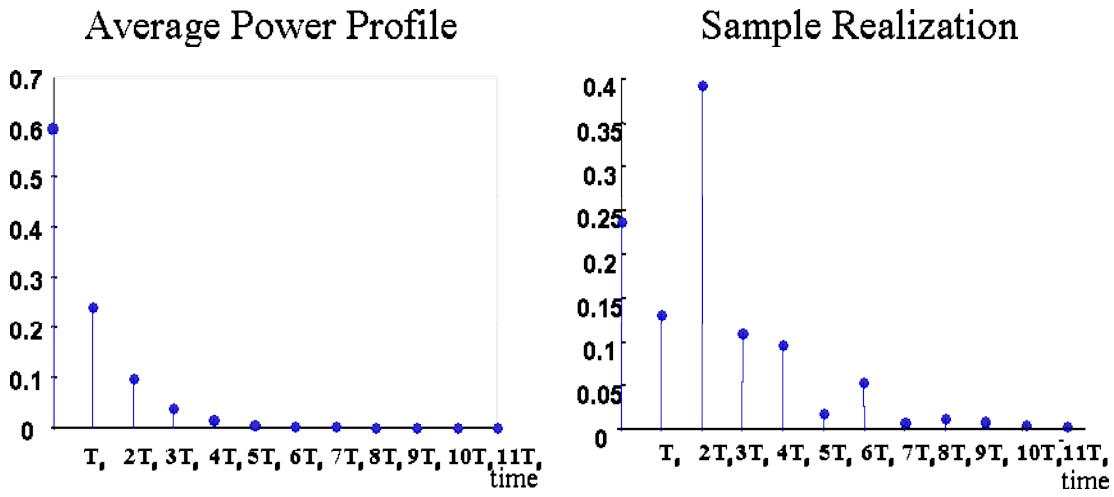

Figure 12. CIR for Exponential Model (From Ref. [16])

between the averaged power profile and an actual realization of the exponential model. Notice the longest delay actually occurs at the second sampling period, rather than the first.

The normalization factor, σ_0, ensures that the total average power is one. This is done by the way the σ_0 is chosen. The model is normalized so that the expected value power gain of the ensemble is equal to zero decibels (dB), even though an individual

realization's power gain may not be equal to zero [15]. Since this is not the same as producing the channel model and forcing each realization to have zero average power gain, the model includes intersymbol interference (ISI) and flat fading [16]. The existing exponential channel model is normalized in the expected value sense [15]

$$E\left\{\sum_{k=0}^{k_{\max}}|h_k|^2\right\}=\sum_{k=0}^{k_{\max}}\sigma_k^2=\sigma_0^2\sum_{k=0}^{k_{\max}}e^{\frac{-kf_s}{\tau_{ms}}}=\sigma_0^2\frac{1-e^{\frac{-(k_{\max}+1)f_s}{\tau_{ms}}}}{1-e^{\frac{-f_s}{\tau_{ms}}}} \tag{0.14}$$

$$\Rightarrow\sigma_0^2=\frac{1-e^{-\frac{f_s}{\tau_{rms}}}}{1-e^{-\frac{(k_{\max}+1)f_s}{\tau_{rms}}}}=\frac{1-\beta}{1-\beta^{k_{max}+1}}\,.$$

2. Rayleigh Fading Model

As already noted, the Rayleigh distribution is a commonly used technique for multipath channel modeling. The Task Group b proposal includes a means to model Rayleigh, or flat, fading as a special case of the exponential model. Flat fading means the channel affects all signal frequencies the same-it is memoryless.

The Rayleigh fading case is made a limiting case of the exponential model in order to maintain the model's simplicity. To do this the model is made single tap - k_{max} is fixed to one - and the RMS delay spread, τ_{RMS}, is set to zero. The single tap simply scales and rotates the received signal. Therefore, the Rayleigh channel impulse response is

$$h_{Rayleigh}=h_0=N(0,\frac{1}{2}\sigma_0^2)+j\cdot N(0,\frac{1}{2}\sigma_0^2)\,, \tag{0.15}$$

where σ_0^2=1. The variance of the noise used to generate is fixed at 1/2 for the real and imaginary components [16]. All the frequencies are affected the same because multiplication, not convolution, is employed.

Finally, the simulation model includes additive white Gaussian noise, because of its noticeably adverse effect on performance in addition to multipath fading.

B. RICIAN FADING

When considering an outdoor environment, the Rayleigh distribution model may not prove to be adequate because it does not take into account the possibility of a dominant line of sight component. The Rician model does. The simplicity of the exponential model and the limiting case of the Rayleigh within it notwithstanding, a slightly more complex model is required to describe the Rician fading case. Still, the advantages of the exponential model can still be applied.

Rician fading is then the result of the presence of a dominant component plus diffuse component; Rayleigh fading is the result of only the diffuse component.

Recall the entire received signal is

$$r(t) = A_0 p(t) + \sum_{i=1}^{N} A_i p(t - \tau_i) . \tag{0.16}$$

A_0 is the amplitude of the dominant component and A_i is the amplitude of a multipath component. In the exponential model the expected value normalization is one to ensure the average power gain is zero dB. In other words, the sum of the power of the diffuse components equals one. With the addition of a dominant component, the total average power gain must remain zero dB, i.e., where the diffuse components are adjusted in magnitude to reflect the addition of the dominant component, while maintaining an overall zero dB average power gain.

$$E\left\{\left|h_{00}\right|^2\right\} + E\left\{\left[\left|h_0\right|^2 + \left|h_1\right|^2 + \left|h_2\right|^2 \ldots \left|h_{k_{\max}}\right|^2\right]\right\} = 1 , \tag{0.17}$$

where h_{00} represents the Rician component power and [·] represents the Rayleigh fading components.

The expected value normalization still depends upon how σ_0^2 is chosen. The total average power gain of the diffuse components must then equal

$$1 - E\left\{|h_{00}|^2\right\} = E\left\{\left[|h_0|^2 + |h_1|^2 + |h_2|^2 \ldots |h_{k_{\max}}|^2\right]\right\}, \tag{0.18}$$

which leads to

$$\sigma_0^2 = \frac{1-\beta}{1-\beta^{k_{max}+1}}\left(1 - E\left\{|h_{00}|^2\right\}\right), \tag{0.19}$$

As noted above, a channel's impulse response is very much affected by the delay spread. Figure 13 illustrates the CIR for a Rician fading channel with a LOS component power of 0.5.

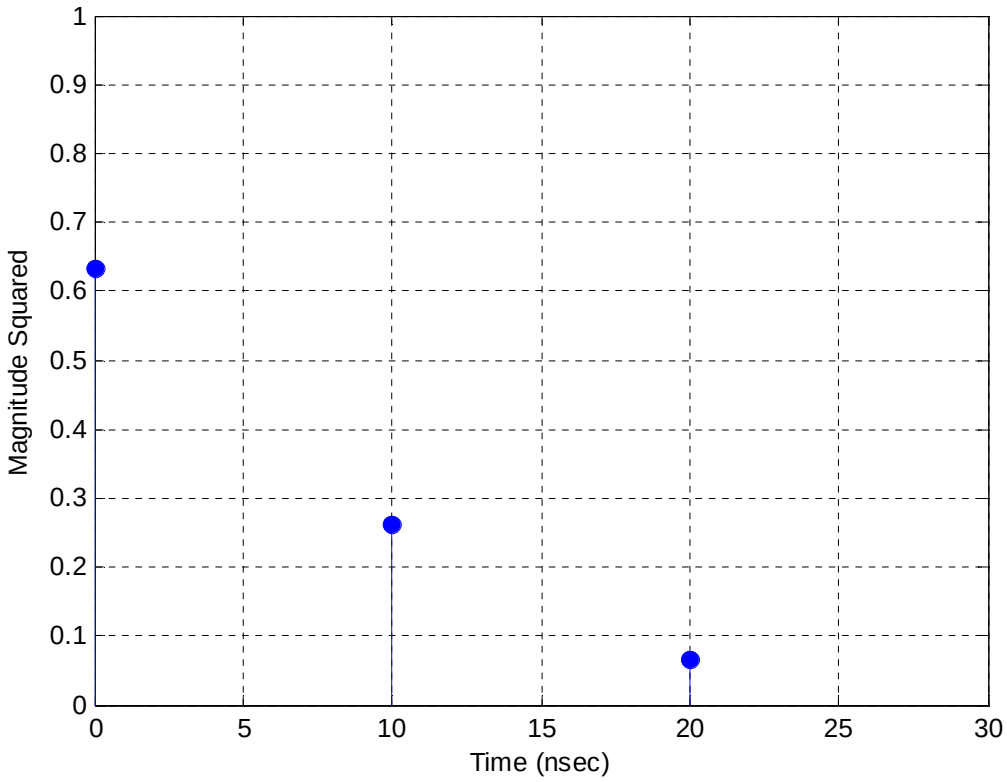

Figure 13. Sample Realization of the CIR for a Rician Fading Channel τ_{RMS}=10 ns, f_s=20 MHz (LOS Component Power=0.5)

Notice how quickly the multipath signal dies out, preventing the possibility of destructive interference causing fading. Also, this is a single realization of the channel so its power gain is not necessarily 0 dB.

When the delay spread increases, more multipath signals interfere with the desired signal. Also, it takes longer for the reflected signals to end. Figure 14 shows another CIR for a Rician fading channel with LOS component power of 0.5.

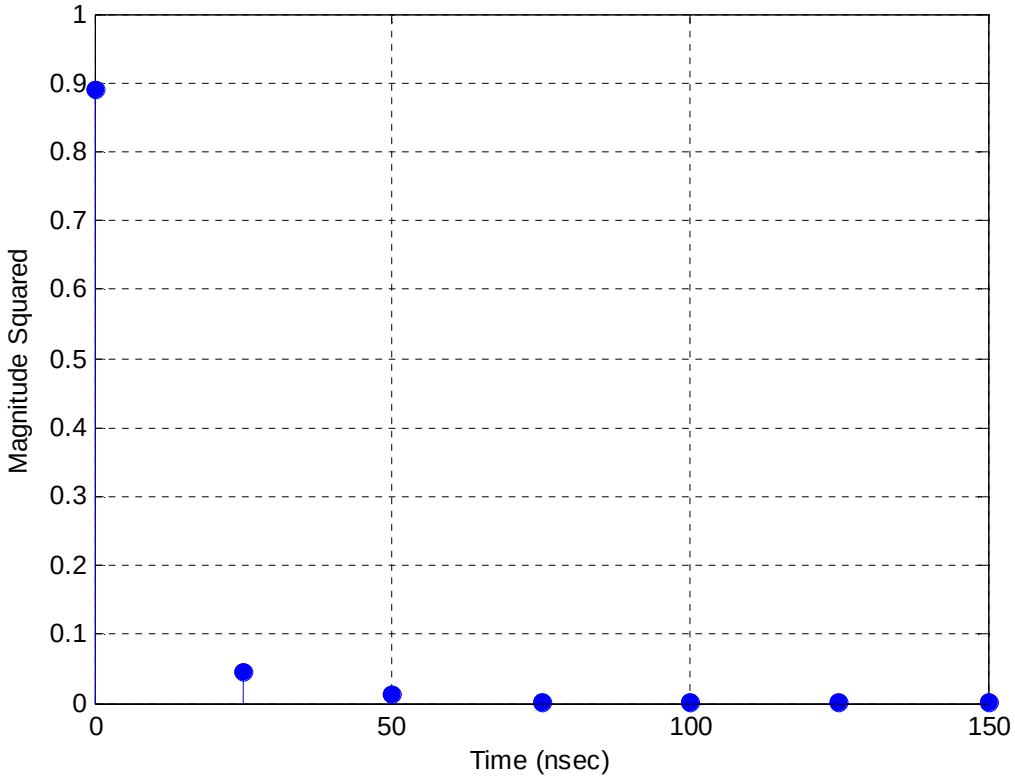

Figure 14. Sample Realization of the CIR for a Rician Fading Channel τ_{RMS}=25 ns, f_s=20 MHz (LOS Component Power=0.5)

This example of a CIR is monotonically decreasing, although, as will be seen below, this is not always the case. The path dies at 125 ns. Although the delay spread was increased by 2.5 times from the previous example, it took over 5 times as long for the signal path to end.

Figure 15 shows a Rician fading channel with a LOS component power of 0.5.

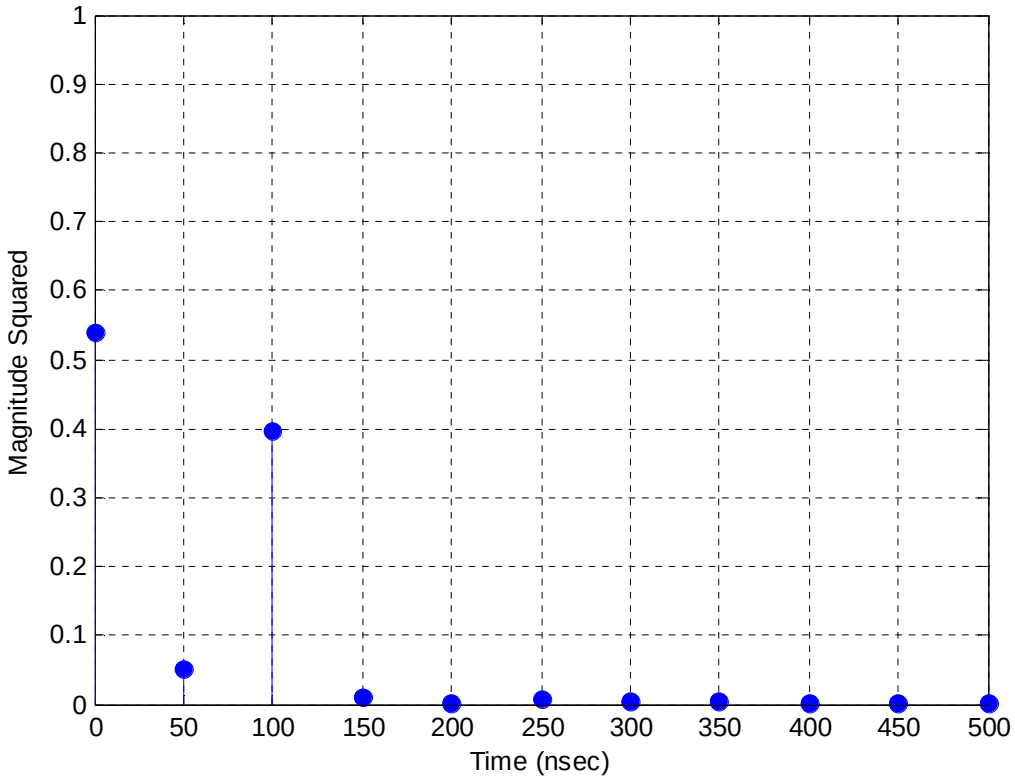

Figure 15. Sample Realization of the CIR for a Rician Fading Channel τ_{RMS}=50 ns, f_s=20 MHz (LOS Component Power=0.5)

Notice the largest path occurs at a delay two sampling periods. The addition of the LOS component only caused a slight increase in the path at four sampling periods.

Figure 16 illustrates a Rician fading channel at a delay spread of 75 ns with a LOS component power of 0.5.

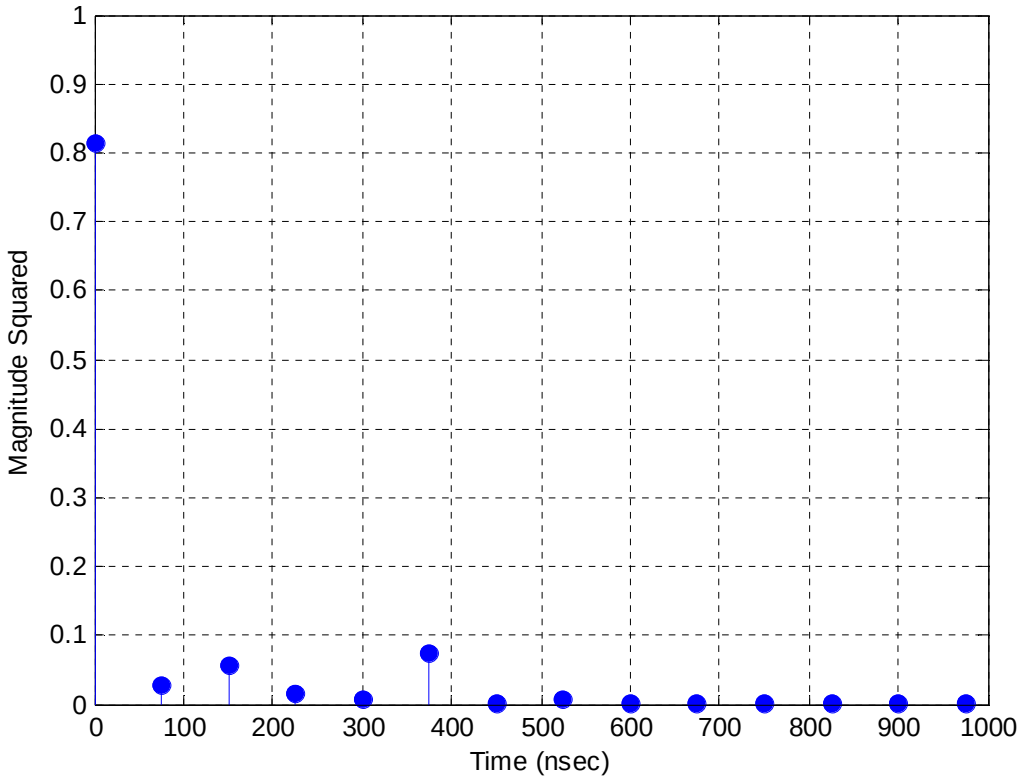

Figure 16. Sample Realization of the CIR for a Rician Fading Channel τ_{RMS}=75 ns, f_s=20 MHz (LOS Component Power=0.5)

The largest path occurs at 75 ns. Notice the CIR is not a smoothly declining curve. It takes longer for the response to end, with the impulse not ending until 900 ns.

Figure 17 illustrates a CIR with a delay spread of 100 ns. Again notice the increase in time before the single begins to significantly small.

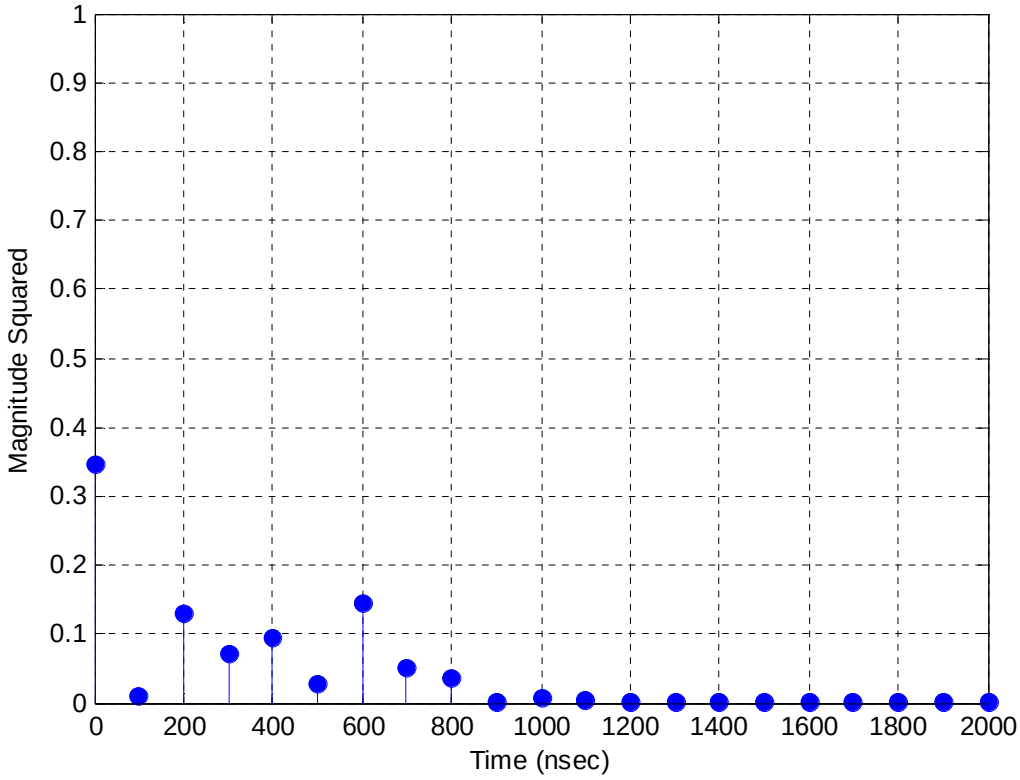

Figure 17. Sample Realization of the CIR for a Rician Fading Channel τ_{RMS}=100 ns, f_s=20 MHz (LOS Component Power=0.5)

Notice several paths are of nearly equal value and at the 600 ns the path delay is still fairly large. At 900 ns the path finally ends.

The exponential channel model provides a robust model that allows for the simulation of a Rician fading channel with varying RMS delay spreads.

C. COCHANNEL INTERFERENCE

Cochannel interference (CCI) refers to interference from another channel utilizing the same frequencies. CCI can be introduced in a number of ways including: accidental transmission, radiation spillover from an antenna sidelobe, or by other authorized users of the same spectrum. The latter cause of CCI presents a significant problem for mobile phone communication engineers and operators of wireless LANs. Currently, IEEE 802.11a standard operates in the Unlicensed National Information Infrastructure (U-NII)

band, which is a part of the radio spectrum reserved by the Federal Communications Commission (FCC) and provided to manufacturers of radio frequency equipment without a license. With the use of the spectrum widely available, the possibility of CCI is very high.

Much of the literature on modeling of CCI is experimental. In the real world it is difficult to determine what may cause interference. Although the FCC has stipulated some limitations on transmit power, wireless LANs exist everywhere and many within close proximity to each other. For the purpose of this channel model, the cause of CCI was modeled as a similar OFDM signal with a phase angle randomly chosen and uniformly distributed from 0 to 2π.

D. SUMMARY

This chapter discussed different aspects of the wireless channel model. In particular it focused on the multipath nature of this channel and the challenges it presents for modeling. Ultimately, the exponential channel model was chosen with a limiting case for Rayleigh fading and an adjustment for Rician fading. Finally, CCI and its implementation were discussed.

The next chapter discusses the simulation methodology, the simulations conducted and presents an analysis of the results.

IV. PERFORMANCE AND ANALYSIS

OFDM provides a robustness and spectral efficiency in wireless communications that make it very appealing. Its performance in AWGN is very good. In lower SNR the distortion of the signal increases. To combat this phenomena channel coding is utilized. Both hard-decision decoding (HDD) and soft-decision decoding (SDD) may be used. HDD and SDD achieve coding gains of 3 dB and 6 dB, respectively [5].

In a multipath fading environment, even with channel coding, perfect frequency and time synchronization, the bit error rate is fairly high. To overcome this, equalization is applied at the receiver. An estimate of the channel's impulse response (CIR) at the receiver simply divides the received signal in the frequency domain. Obviously, this technique's utility is directly connected to the accuracy of the estimated CIR at the receiver. Also, in some samples equalization increases the noise [5]. The question remains as to how OFDM fares under more severe channel conditions, e.g. cochannel interference and lower SNR.

A. MODEL FLEXIBILITY

As noted above, the exponential channel model presents a very simple but realistic means of modeling a multipath fading channel. In order to illustrate the performance of the model under different LOS component power values, a simulation was run with perfect synchronization and equalization. The LOS power values range from zero to one, that is, from Rayleigh fading to AWGN. Figure 18 illustrates the progression of the simulation model through different LOS component power values. The simulation was run at 12 Mbps, that is with QPSK, with an RMS delay spread of 75 ns and coding rate R=1/2.

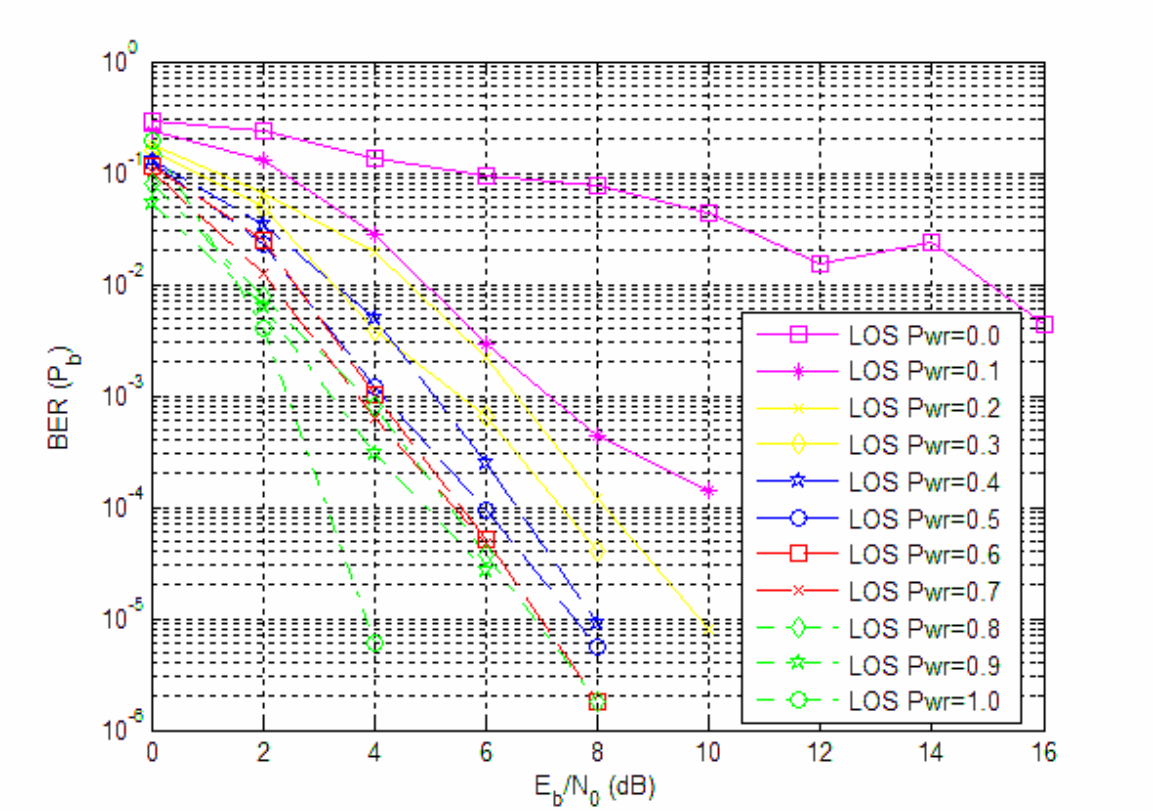

Figure 18. Performance of IEEE 802.11a 12-Mbps Mode, Rician Fading

The power is incremented in tenths from zero to one. When the LOS component power equals 0, the model is essentially Rayleigh. However, when the LOS component power equals 1, the model resembles AWGN. Figure 18 shows a clear depiction of the model's robustness.

B. PERFORMANCE IN RAYLEIGH AND RICIAN FADING WITH CCI

To compare the effects of Rician fading and AWGN on an OFDM signal, two simulations were run with perfect synchronization at 16 dB. Figure 19 illustrates the effect of a Rician fading environment with no CCI on an OFDM signal. The selected data rate was 12 Mbps, which equates to quadrature phase shift keying (QPSK) modulation with R=1/2 coding rate. SDD with weighted decisions was also used to increase performance. Although spreading caused by the distortion of the signal caused by fading is evident, the QPSK constellation is still clearly recognizable.

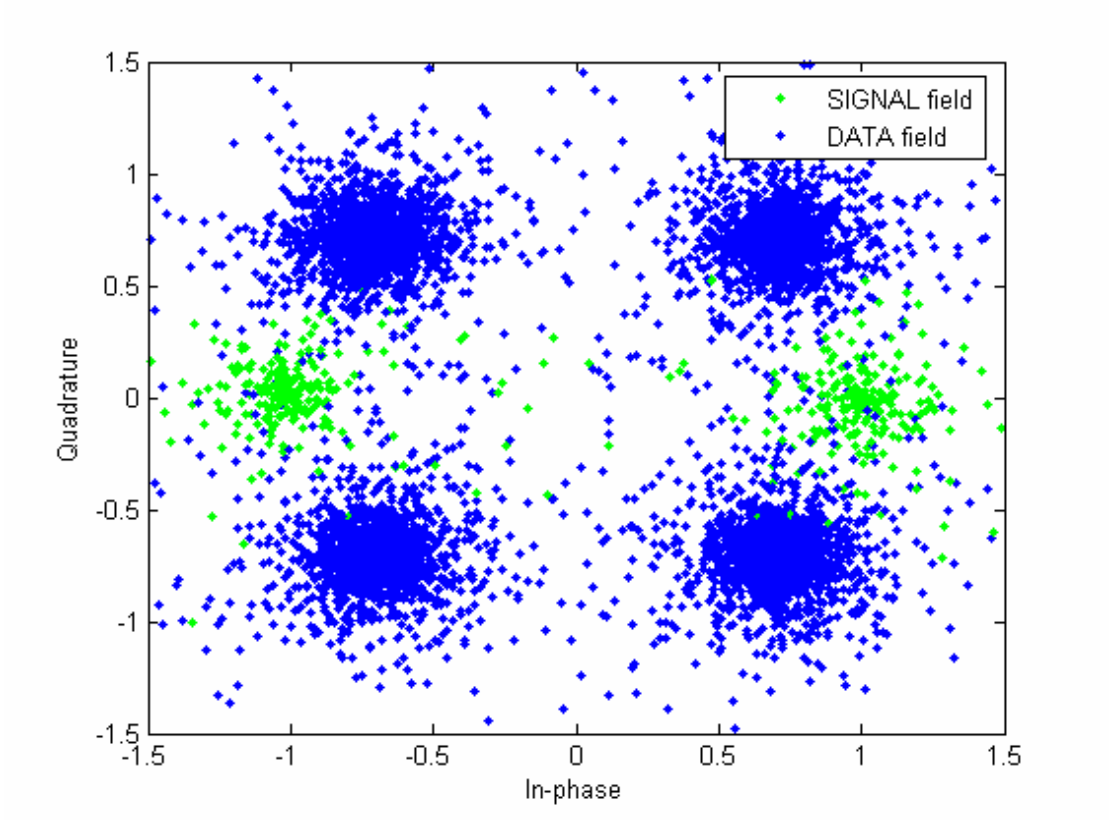

Figure 19. Subcarrier Constellation at the Demodulator (SNR=16 dB, Rician LOS component power=0.6)

The green dots indicate the constellation distortion of the SIGNAL symbol, which is BPSK modulated. The blue dots indicate the DATA symbols.

Figure 20 depicts the AWGN case. Notice the tightly clustered data points in the QPSK constellation. There is far less spreading of data points making demodulation easier and increasing performance.

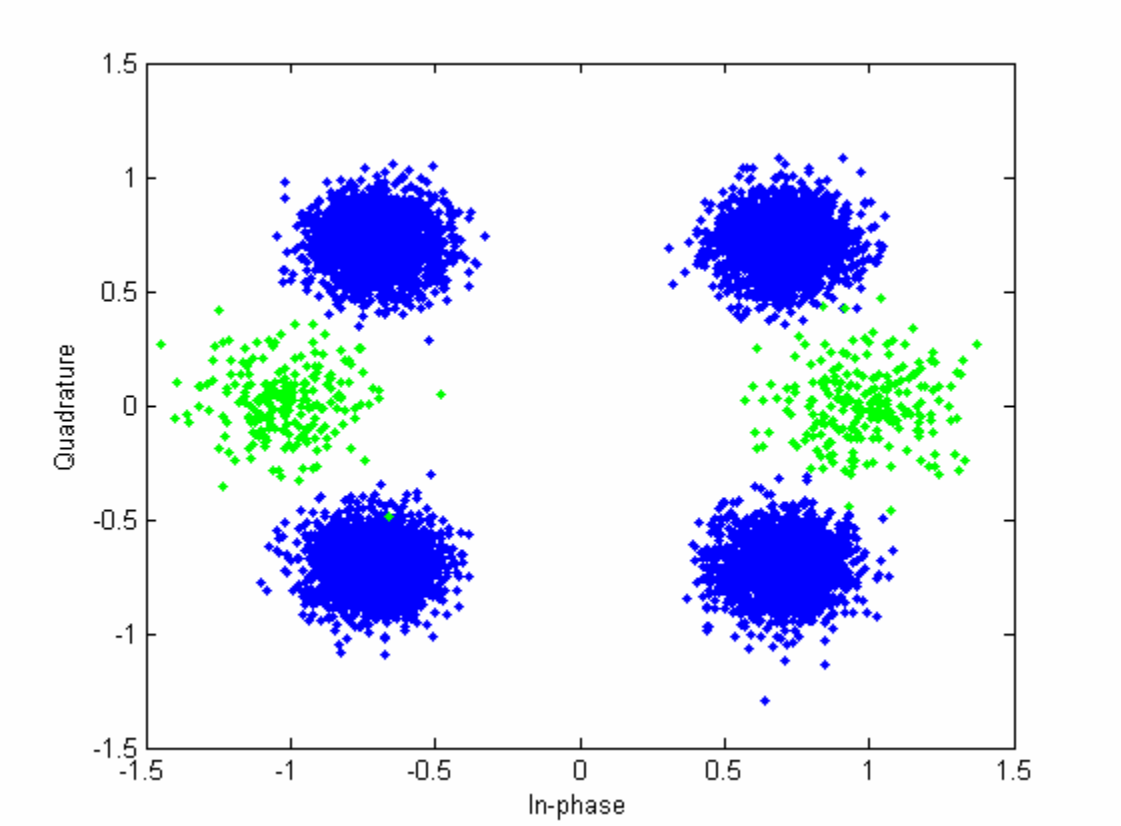

Figure 20. Subcarrier Constellation at the Demodulator (SNR=16 dB, AWGN)

1. Rician Fading with Cochannel Interference

One of the primary impediments to good system performance is CCI. CCI is difficult to quantify and may arrive at the receiver with many different power levels. In order to determine the likelihood of detecting an OFDM signal in this environment, a simulation was run with perfect synchronization and soft decision decoding. Figure 21 shows the results using τ_{RMS}=75 ns.

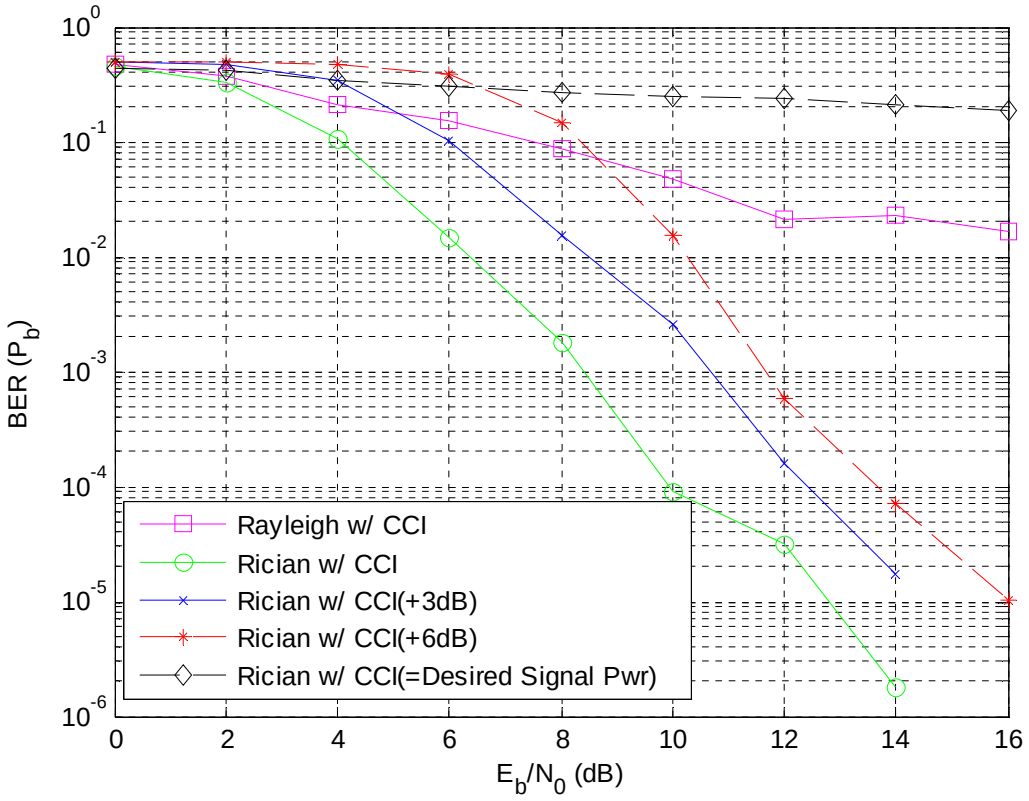

Figure 21. OFDM Signal in Rayleigh and Rician Fading w/ CCI (QPSK, R=1/2, τ_{RMS}=75 ns, LOS Component Power=0.5)

Taking the desired QPSK signal and randomly changing the phase forms the CCI. The power in the phase-changed signal is then measured and added to the desired signal along with the AWGN. In the Rayleigh fading and the first Rician fading, the CCI is adjusted, like the AWGN, for increasing values of signal power to reflect an increasing SNR. In the third curve, the CCI was increased by 3 dB. In the fourth curve, the CCI was increased by 6 dB. In the final curve, the CCI power was set equal to the desired signal power. The last three curves illustrate CCI from a source consistently stronger than the desired signal. Also, the LOS power component was held constant throughout all the simulations.

The performance of the receiver in the presence of CCI is not feasible for most realizable systems. As expected, the simulation with the least amount of CCI performs the best, but that performance is not acceptable until the signal's E_b/N_o reaches 16 dB.

Note also that when the CCI power equals the desired signal power the, the desired signal is unrecoverable.

Also of interest is the ability to receive and accurately demodulate a signal at some of the various data rates available in the IEEE 802.11a standard. This simulation was run with perfect synchronization and soft decision decoding. Again, the CCI power was adjusted for increasing values of desired signal power and the RMS delay spread was 75 ns.

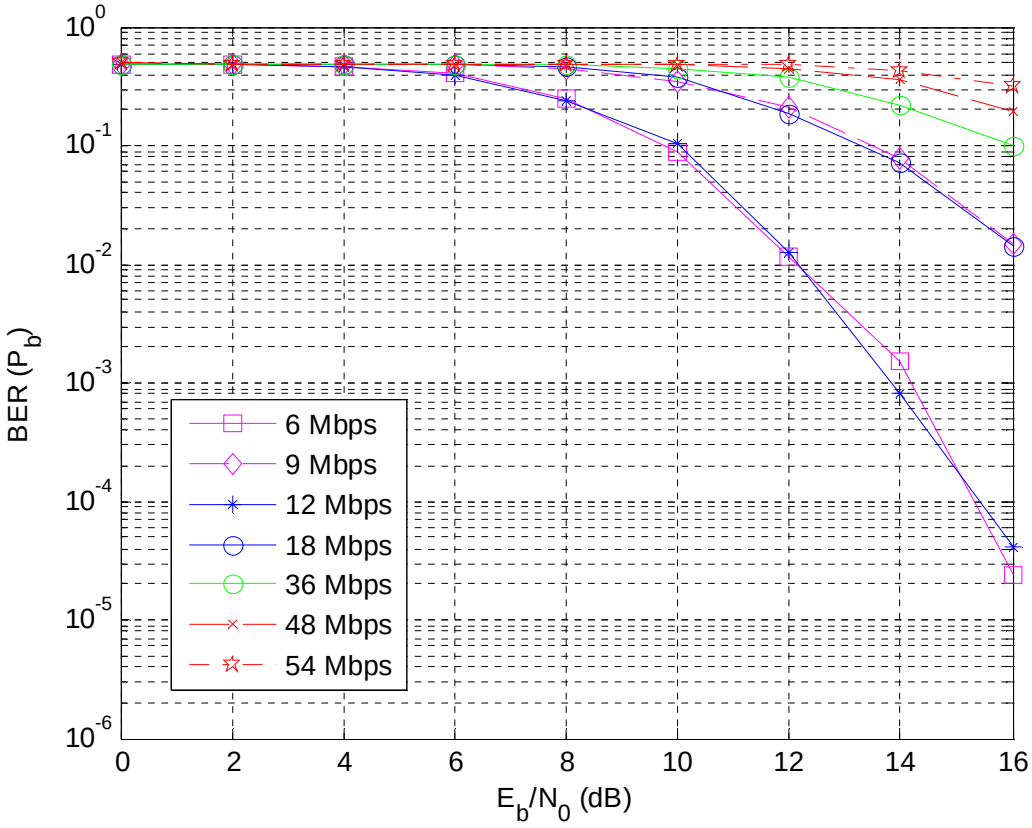

Figure 22. OFDM Signal in Rayleigh and Rician Fading w/ Varying CCI (τ_{RMS}=75 ns)

Figure 22 displays the results. Clearly the more robust data rates, that is, those at 6 and 9 Mbps, do the best. This is achieved at the cost of throughput. Data rates of 6 and 12 Mbps are BPSK and QPSK, respectively, with coding rate R=1/2. Data rates of 9 and 18 Mbps are also BPSK and QPSK, respectively, but with coding rate R=3/4. These modulation schemes achieve nearly the same performance in constant CCI as in AWGN.

Data rate of 36 Mbps is modulated with 16 QAM at a coding rate of R=3/4. 64 QAM is used for 48 and 54 Mbps at coding rates of R=2/3 and R=3/4, respectively. As the data rate increases, the performance decreases, until at 54 Mbps the signal is unrecoverable with any reliability.

Additionally, a simulation was run to illustrate the effect of CCI on the OFDM signal when the CCI power is equal to the desired signal power, but with different LOS component power. Only two powers were used for the specular component, 0.5 and 1. These values equate to a LOS component half as strong as all the multipath components received and a single LOS component, respectively. Figure 23 shows the results.

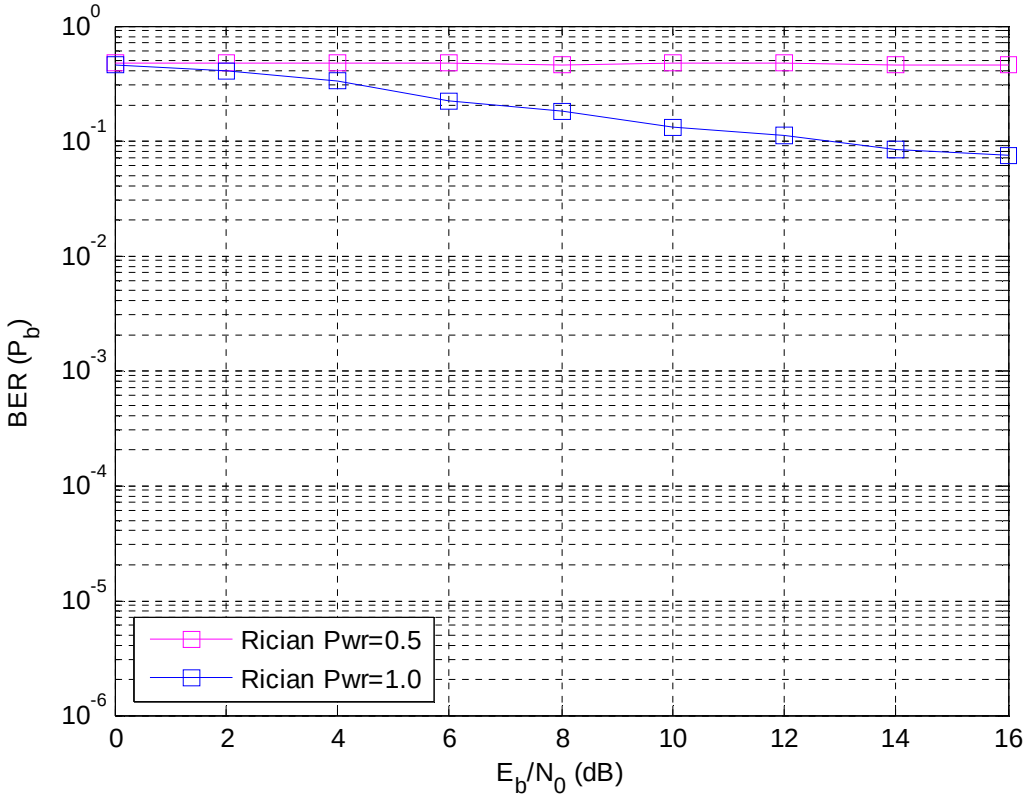

Figure 23. OFDM Signal in Rician Fading w/ CCI Equal to Desired Signal Strength (QPSK, R=1/2, τ_{RMS}=75 ns)

Although there is a spike in bit error rate (BER) at 14 dB, the signal is not feasibly recoverable until about 12 dB with the LOS component as the only component. When the LOS component is set at 0.5, the signal is unrecoverable.

2. Performance of BPSK and QPSK Modulation Techniques

When evaluating the feasibility of recovering a signal, it is useful to evaluate the performance of the different modulation techniques available in the IEEE 802.11a standard. The varied LOS component power used in the simulations for this section were 0, which is Rayleigh, 0.2, 0.5, and 0.8. As noted above, a LOS component power of 1 equates to AWGN.

The IEEE 802.11a standard allows data rates of 6 Mbps and 9 Mbps using BPSK. The 6 Mbps data has a coding rate of R=1/2, while the 9 Mbps has a coding rate of R=3/4. Figure 24 contains the results for BPSK modulation with a data rate of 6 Mbps.

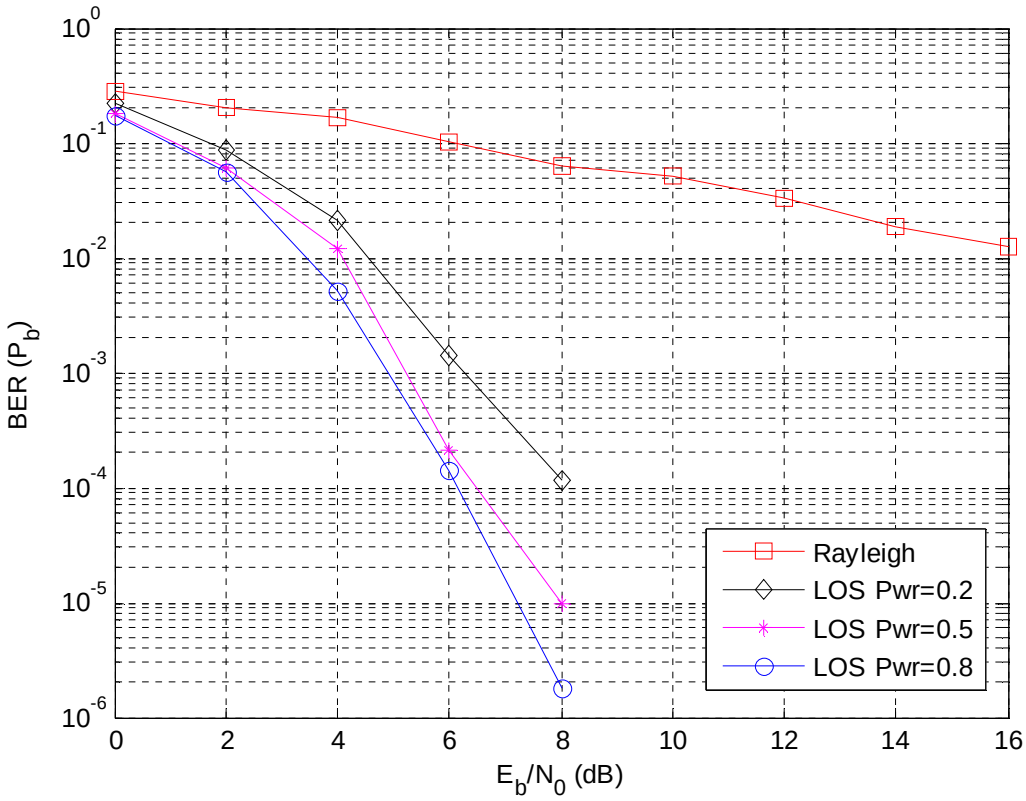

Figure 24. OFDM Signal in Rician Fading at 6 Mbps (BPSK, R=1/2, τ_{RMS}=75 ns)

The Rayleigh fading case with no LOS component indicates extreme difficulty with demodulation. The ability to detect the signal becomes increasingly better as the LOS component power increases. This is to be expected. However, at 6 Mbps, it is clear that with even a small LOS component the ability to recover the signal increases by several

orders of magnitude. The signal, with a LOS component of only 0.2, has a BER of about 10^{-4} at 8 dB. This is well within the performance of realizable systems.

Figure 25 shows the results of BPSK modulation at 9 Mbps. The coding rate at 9 Mbps is R=3/4.

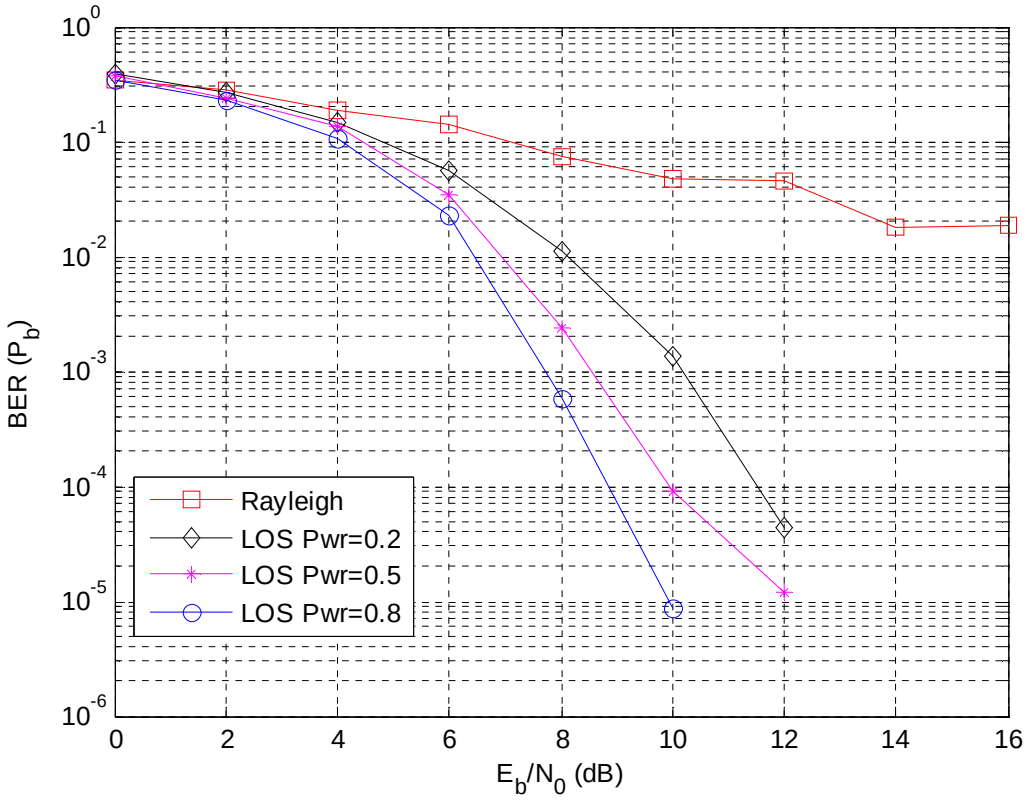

Figure 25. OFDM Signal in Rician Fading at 9 Mbps (BPSK, R=3/4, τ_{RMS}=75 ns)

The performance at this data rate is slightly worse than at 6 Mbps. Again, notice at this very low data rate that even a small LOS component, i.e. 0.2, makes the performance well within the parameters of realizable systems.

QPSK is another modulation technique utilized in the 802.11a standard. This modulation technique is used for data rates of 12 Mbps and 18 Mbps, with coding rates of 1/2 and 3/4, respectively. Figure 26 contains the results for a 12 Mbps data rate.

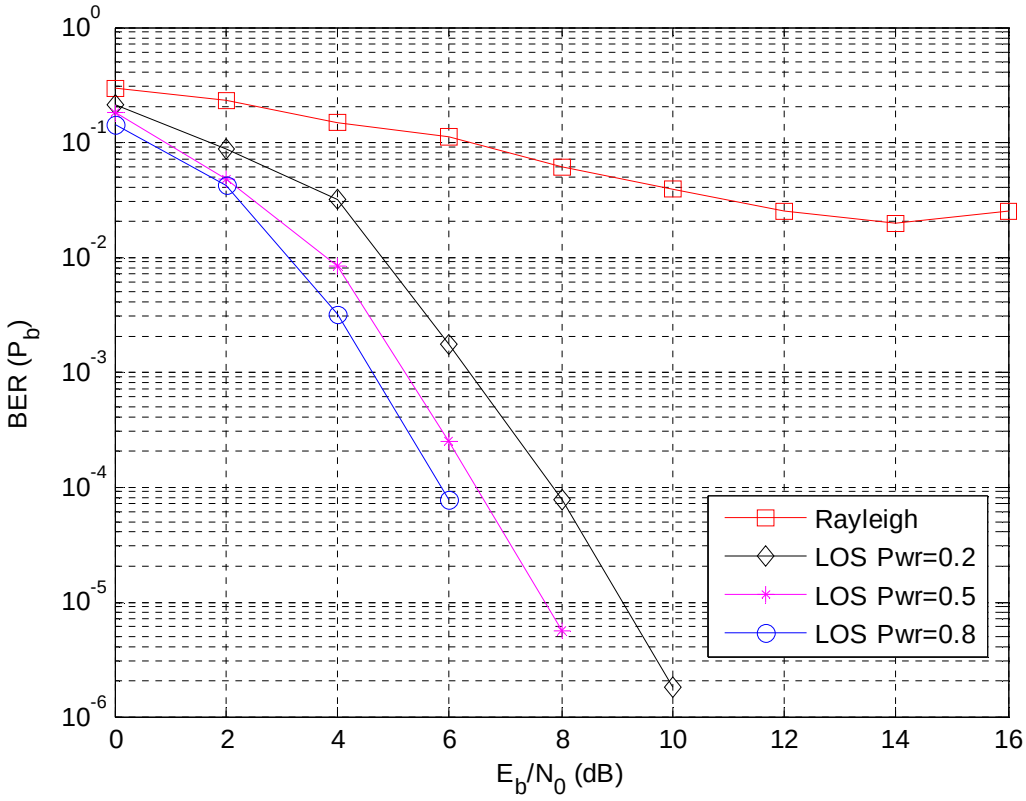

Figure 26. OFDM Signal in Rician Fading at 12 Mbps (QPSK, R=1/2, τ_{RMS}=75 ns)

Although QPSK is more spectrally efficient, its performance is identical to BPSK in AWGN. Here the performance is very close to the 6 Mbps, BPSK performance. Both the LOS power components of 0.2 and 0.5 BER's are identical, but the 0.8 power component is slightly lower.

Figure 27 contains results for QPSK at 18 Mbps.

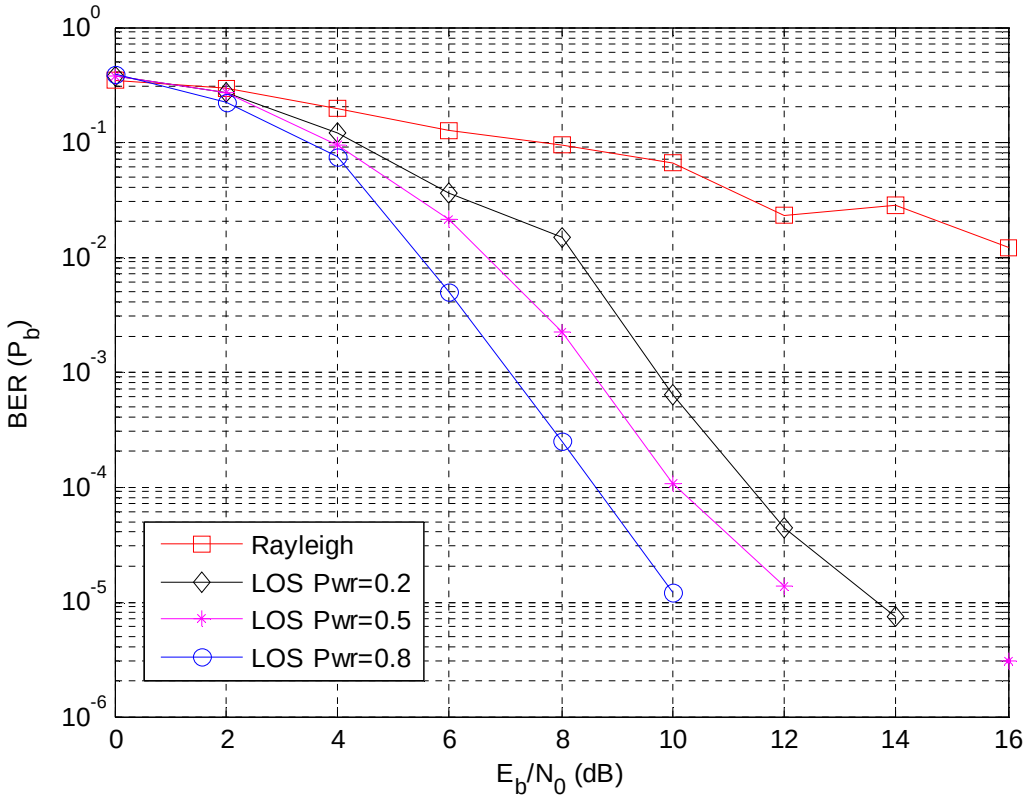

Figure 27. OFDM Signal in Rician Fading at 18 Mbps (QPSK, R=3/4, τ_{RMS}=75 ns)

There is significant improvement between the 0.5 LOS component power and the 0.8 component power. At an E_b/N_o of 8 dB, the 0.5 signal has a BER of $2x10^{-3}$, while the 0.8 signal has a BER $2.5x10^{-4}$. Again, as noted above, these values are all well within the parameters of a realizable system.

3. Performance of 16-QAM and 64-QAM Modulation Techniques

The 16-QAM modulation technique supports 24 and 36 Mbps data rates in the IEEE 802.11a standard. The 24 Mbps data rate has a coding rate of 1/2 and the 36 Mbps data rate has a coding rate of 3/4. Figures 28 and 29 show the results of these two data rate simulations.

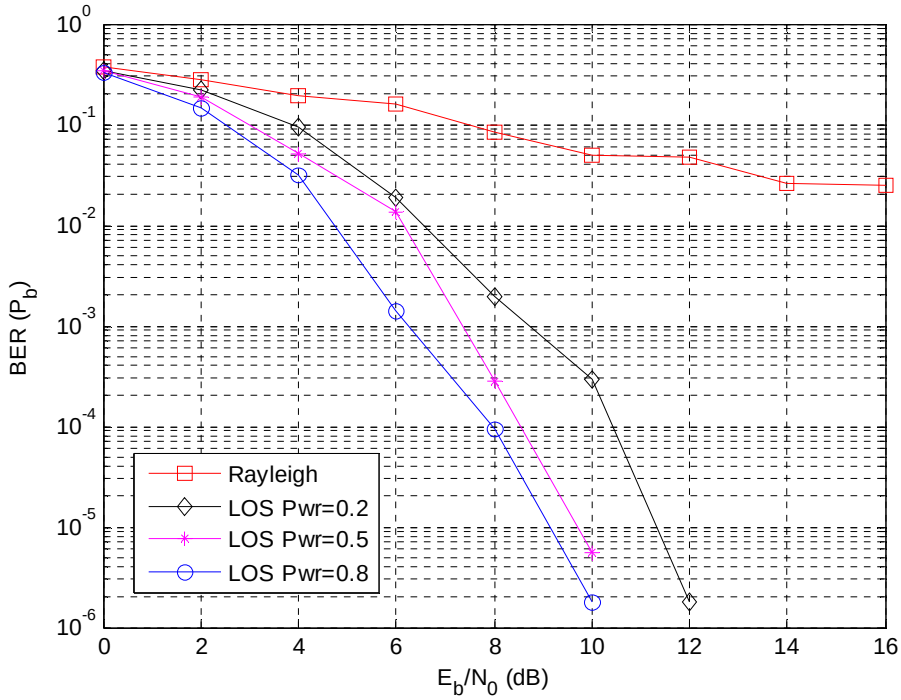

Figure 28. OFDM Signal in Rician Fading at 24 Mbps (16-QAM, R=1/2, τ_{RMS}=75 ns)

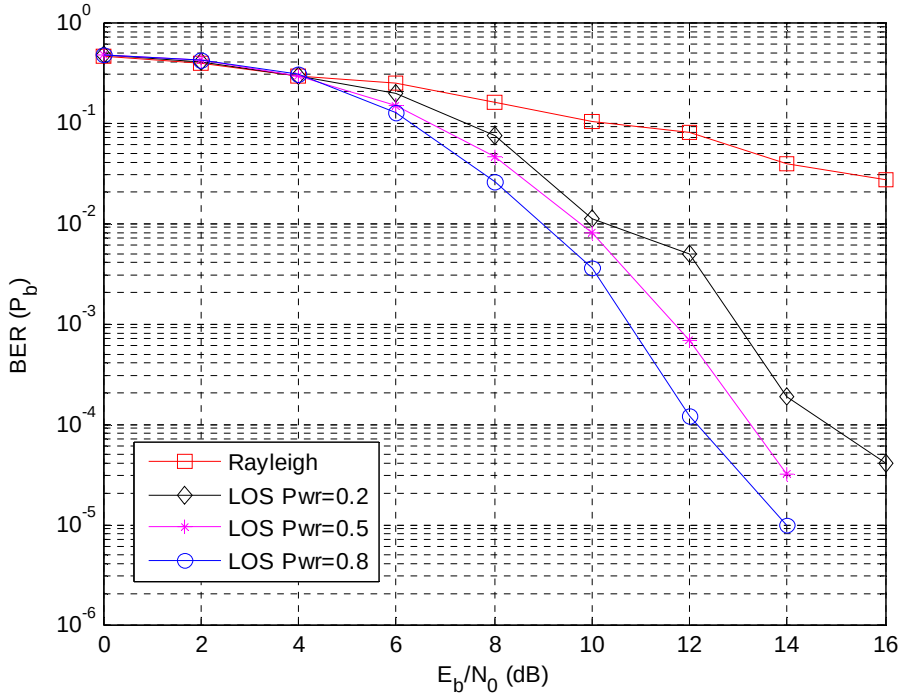

Figure 29. OFDM Signal in Rician Fading at 36 Mbps (16-QAM, R=3/4, τ_{RMS}=75 ns)

As the throughput increases, the performance decreases significantly. It becomes increasingly difficult to recover the signal as more data is sent. For example, at 10 dB for the signal with a LOS component power of 0.8, the BER's are 1.5×10^{-6} at 24 Mbps and 3.5×10^{-3} at 36 Mbps.

Figures 30 and 31 illustrate the same phenomena for 64-QAM. The data rates

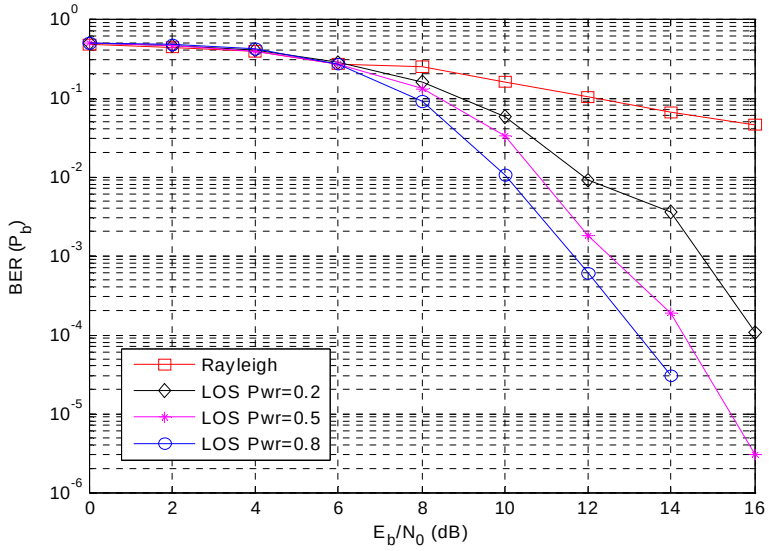

Figure 30. OFDM Signal in Rician Fading at 36 Mbps (64-QAM, R=2/3, τ_{RMS}=75 ns)

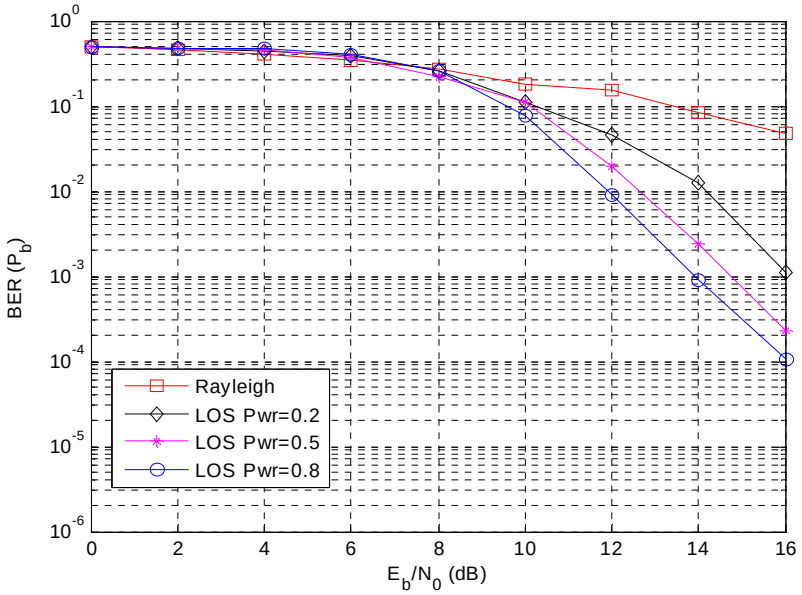

Figure 31. OFDM Signal in Rician Fading at 54 Mbps (64-QAM, R=3/4, τ_{RMS}=75 ns)

supported by 64-QAM are 48 and 54 Mbps, with coding rates of 2/3 and 3/4. 2 dB or more is required to achieve the same performance 48 Mbps and 54 Mbps.

C. RICIAN FADING CHANNEL WITH VARYING RMS DELAY SPREADS

Another impediment to wireless communication, as noted above, is the delay spread of the multipath signals. These signals arrive at times different from each other as well as the original signal and can cause ISI or destructively add due to phase changes. It is useful to consider the effect of various delay spreads on an OFDM signal in a Rician fading channel. The following simulation was conducted with perfect synchronization and soft decision decoding. No CCI was injected. The data rate was 12 Mbps, with QPSK modulation and a coding rate of R=1/2. The LOS component power was set at 0.6. Figure 32 contains the results. An RMS delay spread of 50 ns allows

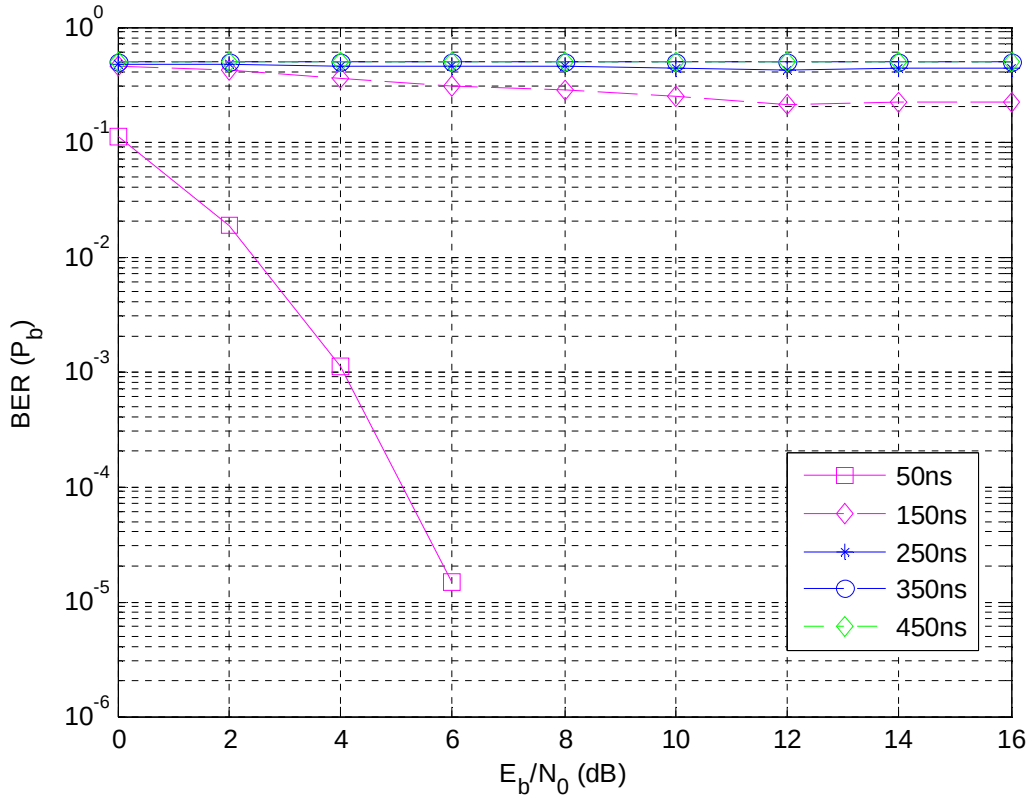

Figure 32. OFDM Signal in Rician Fading with Varying RMS Delay Spread (QPSK, R=1/2)

for excellent performance at E_b/N_o values greater than about 5 dB. The symbol period for an OFDM signal is equal to the guard interval plus the FFT period. In the above figure, the symbol period is 4 μs. As the delay spread approaches the symbol period, the ISI becomes so great as to make the signal unrecoverable.

Figure 33 contains the results of a simulation run with CCI injected in the received signal. All other parameters are the same as Figure 33.

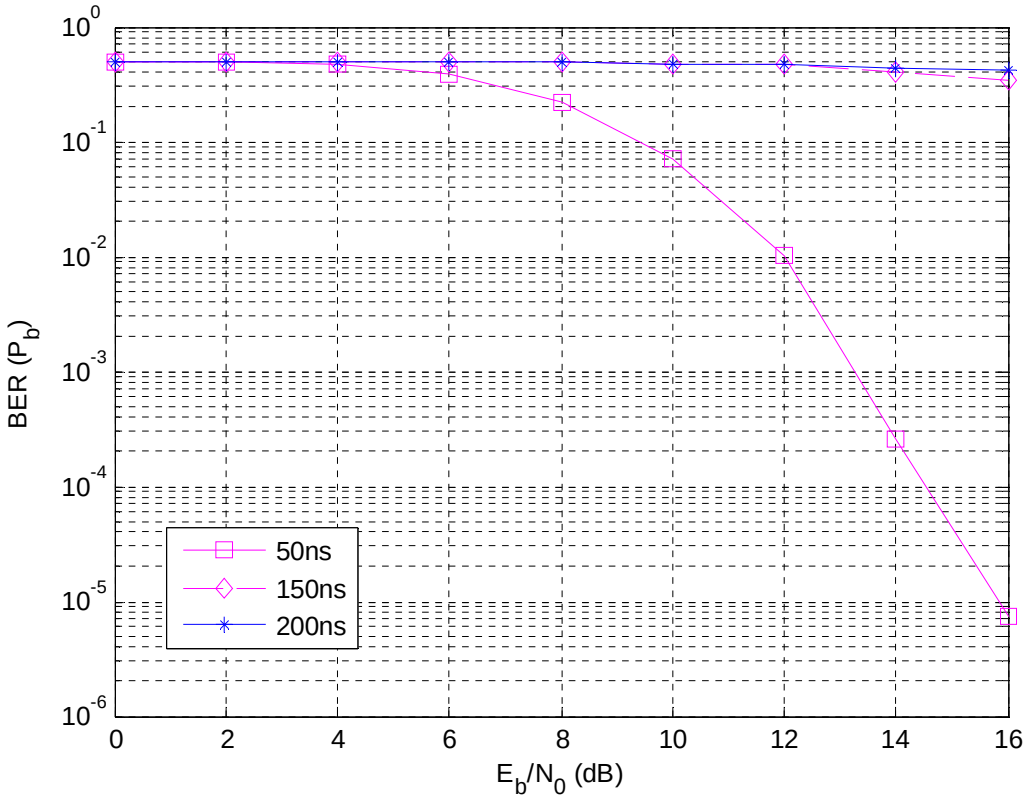

Figure 33. OFDM Signal in Rician Fading with Varying RMS Delay Spread and CCI (QPSK, R=1/2)

As in Figure 21, the CCI is derived from the phase-changed desired signal and is adjusted for increasing SNR. Only three different RMS delay spreads were used for this simulation because of the quickness with which the signal becomes unrecoverable. The CCI greatly decreases the performance even at the more manageable 50 ns delay spread; however, 150 ns is far too much delay spread for the receiver to overcome.

D. SUMMARY

In this chapter the performance of IEEE 802.11a was evaluated under many operational modes. First the flexibility of the channel model was shown. It was noted that the channel model could be used to consider Rayleigh or Rician fading, as well as a straightforward exponential decaying envelope. Cochannel interference was injected into the channel and the performance evaluated. The power of the CCI was adjusted while all other parameters were kept constant, which aided in evaluating the algorithm. Performance was also evaluated under CCI with the different data rates available for the 802.11a standard. Next each operational data rate was evaluated under CCI and Rician fading. Several values were used for the LOS component power and compared. The results show that the performance degrades with increasing data rate with losses ranging from 1 to 4 dB. Finally, a comparison was made of the performance under different RMS delay spreads and the symbol period. Without CCI at 12 Mbps, the signal quickly reached a BER greater than 10^{-1} with τ_{RMS} >75 ns. When CCI was added, the performance became unmanageable even more quickly.

Of note is the assumption of perfect synchronization and accurate channel estimation for all the simulations. Without those factors, the BER remains as high $5x10^{-1}$ for the duration of the simulation. Also, neither frequency nor spatial diversity was included.

The next chapter provides a summary of conclusions by chapter and ideas for future research.

V. CONCLUSIONS AND FUTURE WORK

This thesis presented an evaluation of the performance of orthogonal frequency division multiplexing in an austere environment. A simulation toolbox was modified to allow for the introduction of cochannel interference and low SNR. Also the exponential channel model was modified to include cases for Rician fading. This chapter summarizes the main conclusions and provides suggestions for future work.

A. SIGNIFICANT RESULTS AND CONCLUSIONS

Chapter II introduced the concept of OFDM, including its history and implementation. Its advantages over single-carrier systems were also discussed. The orthogonality of the subcarriers allows for overlapping of frequencies. Adding a guard interval alleviates ISI. A basic schematic of a typical OFDM transmitter and a description of a basic receiver were provided. An overview of the IEEE 802.11a standard addressed the issue of which standard would be simulated for evaluation purposes. The wireless environment was also discussed. Multipath fading and its effects on signal performance were addressed. Finally, a description of the outdoor wireless environment provided insight into the problems with performance that may be encountered.

Chapter III provided an in depth analysis of the channel model utilized for the simulation. The exponential model adopted by the IEEE Task Group b provided the basis for the model. That model accounted for Rayleigh fading and ISI, but did not include provisions for Rician fading, a real possibility in the outdoor environment, and CCI. Although qualitatively it would be expected for performance in Rician fading to be better than performance in Rayleigh fading, it was necessary to show quantitatively the values of BER versus E_b/N_o to determine when the signal becomes unrecoverable. Numerical analysis of the model was done to show how it could be modified to account for both phenomena.

Chapter IV presented performance and analysis of the IEEE 802.11a standard in various operational modes and under various channel conditions. The flexibility of the model was first demonstrated and then the effect of multipath fading on the demodulation

of a signal was shown. The standard was evaluated under Rician fading with cochannel interference where it was found that the greater the LOS component power, the better the performance. As the LOS component power decreased in value, the performance worsened, but was still within the E_b/N_o range of most realizable systems. IEEE 802.11a was also evaluated in the various modulation techniques and data rates available for the standard. This analysis showed that with the increase in data rate, there was a 2 to 4 dB loss. Finally, an evaluation was performed with varying RMS delay spreads under Rician fading and CCI. This showed a precipitous decline in performance as the RMS delay spread became greater than 50 ns. Since outdoor environments typically produce delay spreads in excess of 50 ns, IEEE 802.11a would not work well in outdoor environments unless mitigation techniques are used to discriminate against multipath signals.

B. SUGGESTED FUTURE WORK

There are several areas that ripe for continued research. All simulations in this research were conducted assuming perfect synchronization and accurate channel estimation. While the latter maybe readily done for any receiver, the former is more difficult if the receiver has little knowledge of the transmitter. CCI can be very high and it was shown that when CCI is equal to the desired signal strength, the desired signal is unrecoverable. A way to mitigate CCI with the receiver having little knowledge of the transmitter would be desirable. Finally, the geolocation and tracking of OFDM signals should be explored. Because of its proliferation, the ability to determine the location of a mobile OFDM user would be helpful for both commercial and military purposes.

LIST OF REFERENCES

[1] J. J. van de Beek, P. Ödling, S. K. Wilson, P. O. Börjesson, "Orthogonal Frequency-Division Multiplexing (OFDM)", 2002. http://www.s3.kth.se/signal/grad/OFDM/URISIOOFDM9808.htm, (last accessed November 2005.)

[2] D. Matiae, "OFDM as a Possible Modulation Technique for Multimedia Applications in the Range of MM Waves", *Introduction to OFDM,* 2nd Edition, October 1998.

[3] R. van Nee and R. Prasad, *OFDM for Mobile Multimedia Communications*, Artech House, Boston, 1999.

[4] W. Stallings, *Wireless Communications and Networks*, Prentice-Hall, Inc., Upper Saddle River, New Jersey, 2002.

[5] M. Segkos, "Advanced Techniques to Improve the Performance of OFDM Wireless LAN", Master's Thesis, Naval Postgraduate School, Monterey, CA, 2004.

[6] A. Papoulis, *Probalility, Random Variables, and Stochastic Processes*, 2nd Edition, McGraw-Hill, New York, 2000.

[7] B. O'Hara and A. Petrick, *IEEE 802.11 Handbook: A Designer's Companion*, Standards Information Network IEEE Press, New York, 1999.

[8] IEEE 802.11a, "Wireless LAN Medium Access Control (MAC) and Physical Layer (PHY) Specifications: High Speed Physical Layer in the 5 GHz Band," IEEE Std 802.11a-1999, http://ieeexplore.ieee.org/xpl/tocresult.jsp?isNumber=17645 (last accessed Mar 2005.)

[9] M. Pätzold, *Mobile Fading Channels*, John Wiley & Sons, Ltd., West Sussex, England, 2002.

[10] B. Sklar, *Digital Communications: Fundamentals and Applications*, 2nd Edition, Prentice-Hall, Inc., Upper Saddle River, NJ, 2001.

[11] T. S. Rappaport, *Wireless Communications: Principles and Practice,* 2nd Edition, Prentice-Hall, Inc., Upper Saddle River, NJ, 2002.

[12] R. Janaswamy, *Radiowave Propagation and Smart Antennas for Wireless Communications*, Kluwer Academic Publishers, Norwell, MA, 2000.

[13] P. A. Bello, "Characterization of Randomly Time-Variant Linear Channels," *IEEE Transactions on Communication Systems*, Vol. CS-11, pp. 360-393, December 1963.

[14] K. I. Pedersen, P. E. Mogensen, and B. H. Fleury, "A Stochastic Model of the Temporal and Azimuthal Dispersion Seen at the Base Station in Outdoor Propagation Environments," *IEEE Transactions on Vehicular Technology*, Vol. 49, No. 2, March 2000.

[15] J. Fakatselis, *IEEE 802.11-97/157-r1*, November 1997, http://grouper.ieee.org/groups/802/11/Documents/DocumentArchives/1997-docs/97novp.zip, (last accessed November 2005.)

[16] S. Halford, K. Halford, and M. Webster, *IEEE 802.11-00/282r2,* September 2000, http://grouper.ieee.org/groups/802/11/Documents/DocumentHolder/0-282.zip, (last accessed September 2005.)

INITIAL DISTRIBUTION LIST

1. Defense Technical Information Center
   Ft. Belvoir, Virginia

2. Dudley Knox Library
   Naval Postgraduate School
   Monterey, California

3. Professor Tri Ha
   Naval Postgraduate School
   Monterey, CA

4. Professor Herschel Loomis
   Naval Postgraduate School
   Monterey, CA

5. Mr. Nathan Beltz
   Naval Postgraduate School
   Monterey, CA